Geoderma Regional 19 (2019) e00236

Contents lists available at ScienceDirect

Geoderma Regional

journal homepage: www.elsevier.com/locate/geodrs

Soil diversity and major soil processes in the Kalahari basin, Botswana

Rémy Romanens [a], Federico Pellacani [a], Ali Mainga [b], Richard Fynn [c], Pascal Vittoz [a], Eric P. Verrecchia [a,*]

[a] University of Lausanne, Institute of Earth Surface Dynamics, FGSE – Geopolis, 1015 Lausanne, Switzerland
[b] Van Thuyne-Ridge Research Center, Chobe Enclave, Botswana
[c] Okavango Research Institute, P.O. Box 255, Maun, Botswana

ARTICLE INFO

Article history:
Received 25 February 2019
Received in revised form 16 July 2019
Accepted 17 July 2019

Keywords:
Soil mapping
Termites
Rock Eval pyrolysis
Arenosols
Kastanozems
Chernozems
Phaeozems
Solonchaks
Solonetz
Calcisols

ABSTRACT

The study area of the Chobe Enclave (northern Botswana) is defined as mostly covered by Arenosols in available maps. However, recent explorations of the area showed that soils are more diverse than expected. This is because of complex interactions between current alluvial deposition processes, paleo-environmental effects (ancient alluvial deposition, ancient wind-blown sand deposits) and ongoing hydrological effects and colluvial effects on topographic gradients. An in-depth exploration of both soils and vegetation in the area was conducted with the aim (i) to survey the soil diversity at the Chobe Enclave, (ii) to study soil dynamics and identify the key factors of this diversity, and (iii) to create a soil map based on the analysis of the soil-vegetation relationship. For this purpose, thirty-six soil profiles were extensively described according to the World Reference Base for soil resources. In order to better classify these soils, physicochemical parameters, such as pH_{H2O}, exchangeable cations, and particle size distributions, were measured for a specific set of soils ($n = 16$), representative of their diversity. To assess Soil Organic Matter (SOM) dynamics, samples were studied using Rock Eval pyrolysis. Results show a high soil diversity and heterogeneity with the presence of (i) Arenosols, as expected, but also of (ii) organic-rich soils, such as Chernozems, Phaeozems, and Kastanozems, (iii) salty/sodic soils, such as Solonchaks and Solonetz, and finally (iv) calcium-rich soils, such as Calcisols. Analyses of the different actors driving the soil diversity emphasized the importance of the surficial geology, composed of different sand deposits (red sands/white sands), carbonate and diatomite beds, as well as ancient salt deposits, in which high proportions of exchangeable Na^+ were found, associated with high pH_{H2O} (up to 11.3). In addition, as a parameter, the topography creates a complex hydrological system in the Chobe Enclave and therefore, induces a notable soil moisture gradient. Moreover, this study stressed the key role of termites: not only do they modify physicochemical patterns of soils, but they also decay and incorporate large quantities of fresh plant materials into soils. Finally, the analysis of Organic Matter (OM) showed that the Soil Organic Carbon (SOC) is composed essentially by recalcitrant Organic Carbon (OC) substances, such as charcoal, a common carbon type of tropical soils.

1. Introduction

Soils of Botswana are hardly studied and the rare previous research was mostly conducted at a very large scale (Remmelzwaal and Van Waveren, 1988; De Wit and Nachtergaele, 1990; European Soil Data Center (ESDAC), 2014). In these studies, the Chobe Enclave (northern Botswana) is mainly described as completely covered by Arenosols. However, soils are expected to be much more diverse when considering the multiple actors and the complex microtopography of the region. This diversity is suggested by the changing vegetation pattern, where forests and woodlands on the upper positions alternate with grasslands, in the floodplains. This variety in soil types has been confirmed by preliminary explorations of the area by three of the authors, P. Vittoz, A. Mainga, and E.P. Verrecchia, in 2016 and by Diaz et al. (2019). It seems likely that the large number of factors participating in the soil formation in this area, i.e. hydric conditions, topography, nature of the soil parent material (i.e. aeolian or alluvial), impact of biological activity (termites and plants), as well as fires (natural or caused by arson), must lead to a high soil heterogeneity and diversity.

Moreover, understanding the soil diversity and characteristics is essential, first for land management and use, and second, at a larger scale, to estimate the Soil Organic Carbon (SOC) stocks and their associated carbon dynamics. From a conservation and land use perspective, the

---

Abbreviations: BC, black carbon; CEC, Cation Exchange Capacity; I, I-index following Sebag et al. (2016); OC, organic carbon; OM, organic matter; PC, pyrolysed carbon (Rock Eval pyrolysis parameter); PC1–2, principal component 1 and 2; PCA, principal component analysis; R, R-index following Sebag et al. (2016); RC, residual carbon (Rock Eval pyrolysis parameter); SOC, soil organic carbon; SOM, soil organic matter; Tmax, maximum temperature (Rock Eval pyrolysis parameter); TOC, total organic carbon; WRB, World Reference Base for soil resources.

* Corresponding author.
E-mail addresses: pascal.vittoz@unil.ch (P. Vittoz), eric.verrecchia@unil.ch (E.P. Verrecchia).

https://doi.org/10.1016/j.geodrs.2019.e00236

appraisal of the nature and origin of soils in the Chobe Enclave is critical to understand the ecological parameters of the region, such as the vegetation, the heterogeneity and the forage nutrient status for herbivores; in addition, information is needed to assess wildlife ecology and to develop appropriate conservation strategies. The Chobe Enclave is a key dry season range for migratory buffalo and zebra, which is likely linked to the hydrological, soil, and vegetation patterns and dynamics in the region (Fynn et al., 2014). From a SOC perspective, soils are the second largest C sink after the oceans (38,400 Gt; Kutsch et al., 2009; Schmidt et al., 2011; Stockmann et al., 2013). The quantity of Soil Organic Matter (SOM) differs significantly from one environment to another, and although the content rarely exceeds 10 g kg^{-1} (1%) in Arenosols (Blanchard et al., 2005), it can reach up to 90% in organic rich soils such as Histosols (Troeh and Thompson, 2005).

Therefore, this study aims at (i) the inventory and classification of the diversity of soils in the Chobe Enclave, as well as at (ii) proposing a soil map on the regional scale, which can be linked to variation in vegetation structural and community dynamics and wildlife ecology. Furthermore, the various soils, with their respective characteristics, have been interrelated to the key factors listed above; these factors that drive the soil processes allow (iii) SOC dynamics of the area to be better assessed. In order to tackle these objectives, a reconnaissance field work was performed during winter and early spring 2017. A total of 36 soil profiles were described, and a complete vegetation survey was performed for each of them. Among them, 16 representative soil profiles of the observed diversity were selected for further laboratory analyses. As previous studies were more limited in terms of data harvesting, this combined field and laboratory approach helped to better circumscribe the diversity of pedogenic processes at work in the area.

2. Materials and methods

2.1. Study site

The Chobe Enclave (18° 10′ N, 24° 10′ E) is located in northern Botswana, along the Namibian border and close to Zambia. The area is 1690 km^2 (Jones, 2002; Fig. 1). The Chobe Enclave is part of a large trans-border conservation area, called the 440,000 km^2 Kwando-Zambezi Trans-Frontier Conservation Area (KAZA-TFCA; Pricope et al., 2015). The large region of the Chobe has been protected since 1961, first as a game reserve and then, since 1968, as a national park. However, the study area itself, surrounded but outside of the Chobe National Park, is managed by the Chobe Enclave Community Trust (CETC; Pricope et al., 2015).

2.1.1. Climate

The Chobe Enclave is affected by fluctuations of the Intertropical Convergence Zone (ITCZ), which brings heavy thunderstorms and rain during the wet season, from November to March, and high temperatures, i.e. between 30 and 40 °C during the day, in the dry season, from April to October. It is one of the wettest regions of Botswana, with an average annual rainfall of 650 mm (Jones, 2002; Burgess, 2006). For detailed information on rainfall and temperature dynamics over the annual cycle in the region, see Fynn et al. (2014).

2.1.2. Bedrock and soil parent material

The study area is situated in the Kalahari basin, a continuous sand body of 2.5×10^6 km^2 (Jones, 1980). Sands dunes in the study area were formed during dry events of the late Pleistocene (Haddon and McCarthy, 2005). The parent material of a large part of soils in the

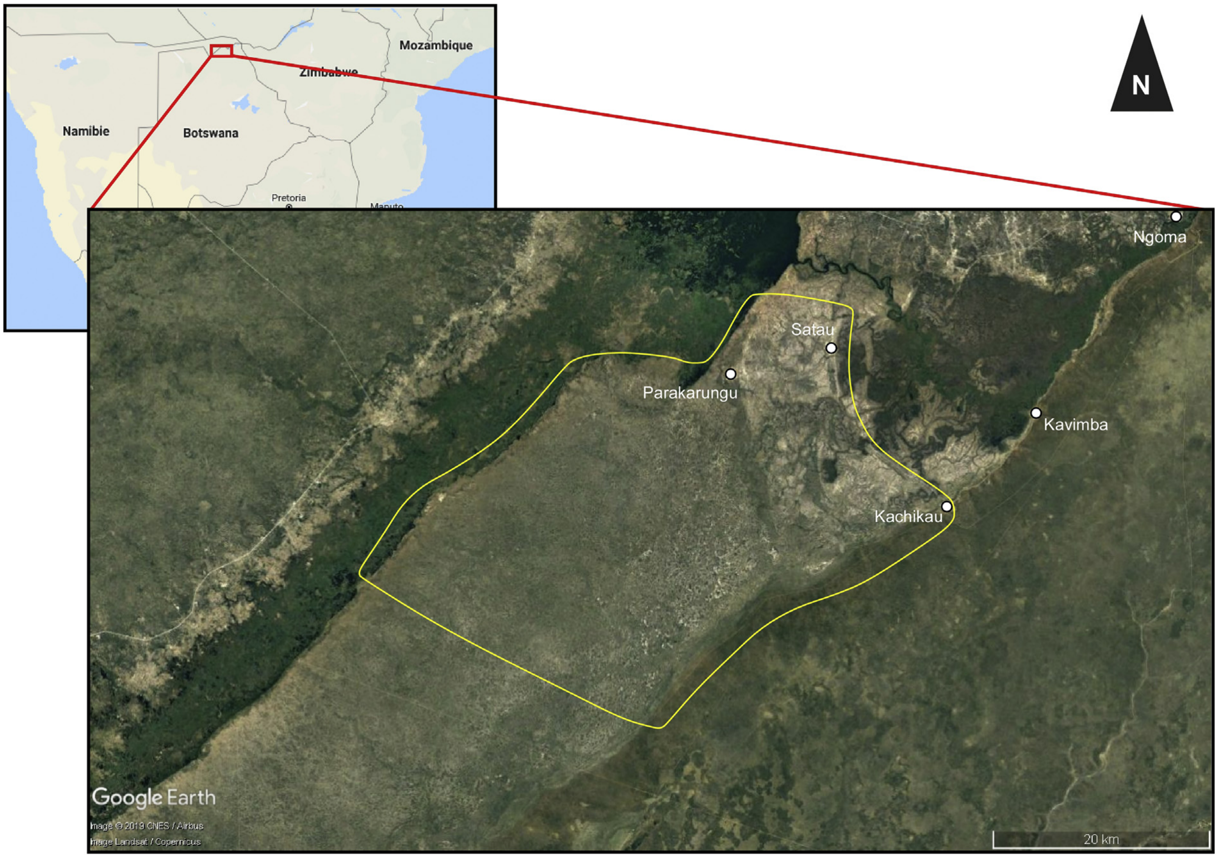

Fig. 1. Situation of the Chobe Enclave in Botswana (upper left map). The soil survey area is delimited by the yellow line. The main villages of the region are located by white dots (modified from Google Map, 2018).

Chobe Enclave directly lie on Kalahari sand deposits (e.g. Wang et al., 2007). Two types of sands were observed: (1) red sands (along the Chobe Fault, and in some places localized within the Enclave), which are deep aeolian sands (McCarthy et al., 2005), and (2) alluvial white sands covering floodplains and infilling paleochannels (Sianga and Fynn, 2017); most of these surficial particles seem to have been reworked by alluvial processes, which have led to the deposition of grey/white sands in the Chobe Enclave depression by the Linyanti River (McCarthy, 2013). In addition, carbonate and diatomite beds were also found outcropping in some places in the central part of the Enclave. They are thought to be ancient palustrine/lacustrine deposits formed during the Quaternary wet periods, when the region was temporally submerged by water (Burrough and Thomas, 2008; Burrough et al., 2009; Diaz et al., 2019; Mendelsohn et al., 2010).

2.1.3. Geomorphology and topography

The Chobe Enclave is clearly limited topographically by two main fault-line scarps belonging to the Okavango Rift Zone (ORZ), which is a western branch of the East-African Rift: (i) the Linyanti Fault (in the northwest) and the Chobe Fault (in the southeast; McCarthy, 2013). In addition to these faults, the area has an extremely complex geomorphology system composed of fossil sandbanks, islands, channels, and swamps. It is composed of an ancient system of islands and channels, which can be easily observed from satellite images. Indeed, the Chobe Enclave is thought to have been part of a large delta and a lake during the Late Pleistocene (Burrough et al., 2009). The formation of some of the islands can probably be compared to those of the present-day Okavango delta system (McCarthy et al., 2012), in which siliceous, low carbonate, and salt deposits occur due to evapotranspiration processes and aeolian dust deposition behind tree curtains (Humphries and McCarthy, 2014). In addition to this microtopography, the region shows a small difference in elevation between extremities (~10 m, with a E-W average slope of 0.025%); large areas of the north-east of the Enclave are regularly flooded by the Linyanti river, whereas the south-west is slightly higher without any flooding, except for small depressions accumulating water after heavy rains (Kinabo et al., 2007). Different geomorphological areas have been recognized in the Chobe Enclave, based on the observation of satellite images and field work. The first one covers the north-east and is mainly composed of grey-white sands, which probably have a fluvial origin, either brought by the Zambezi or by the Linyanti (to a lesser extent) rivers. A second zone, dominated by dark red and reddish sands, stretches all along the Chobe Fault, adjacent to the Chobe Forest Reserve. Finally, the central part of the Enclave, covered by fossil islands and a channel system, is divided into two subareas, a humid one in the north-east (possibly related to floods from the Linyanti and the Zambezi), and a dry one in the south-west.

2.1.4. Vegetation

A large-scale vegetation map, covering the whole North of Botswana, shows that the Chobe Enclave includes mopane forests (dominated by *Colophospermum mopane*), acacia grasslands and sandvelds (low cover of *Acacia* sp., *Terminalia sericea* or *Philenoptera nelsii* on different grass communities), Baikiaea forests (dominated by *Baikiaea plurijua, Baphia massaiensis, Croton gratissimus*) along the southern edge, with riparian forests along the Linyanti and isolated dry floodplains and wetlands in the north-east (Sianga and Fynn, 2017).

2.1.5. Fauna

Termites are known to have an extensive impact on soil proprieties of tropical areas as they modify the soil structure and its clay and SOM contents (McCarthy et al., 1998; Jouquet et al., 2007, 2011; Menichetti et al., 2014). In northern Botswana, three main families of termites have the most impact on soil proprieties: the harvester termites (Family *Hodotermitidae*), the snouted termites (*Trinervitermes* spp., Family *Termitidae*) and the fungus-growing termites (Family *Macrotermitinae*; Gutteridge and Reumerman, 2011). The area is also known for its large populations of big mammals such as elephants, buffalos, and zebras, which can act as geomorphological and soil agents (Butler, 1995; Haynes, 2012; McNaughton et al., 1997).

2.2. Soil description and sampling

Due to the size of the area and the diversity/heterogeneity of the landscape, the sampling strategy was based on an unsupervised vegetation map of the area. This map was created using six wavelengths from Landsat™ images over three seasons (bands 2 to 7: blue, green, red, near-infrared and two bands of short-wave infrared). Sampling sites for soil descriptions were chosen mainly according to the vegetation map and Google Earth images. These sites were selected in order to represent diversities of the vegetation, the substratum, and the geomorphology encountered in the Chobe Enclave. All profiles were situated at a distance < 400 m from the tracks, for safety and time reasons; moreover, spots of relatively homogeneous vegetation and geomorphology were preferentially chosen in order to get representative soil and vegetation surveys. Indeed, each soil description was simultaneously conducted with the description of its associated plant community. Most of the sites retained have been distributed in the central part of the Chobe Enclave because of time and weather constraints (heavy rains in January–February 2017; Fig. A.1).

Thirty-six soil profiles were dug at a minimum depth of 80 cm and up to 140 cm. Samples were collected systematically at fixed depths: 0–5 cm, 10–15 cm, 25–30 cm, 45–50 cm, 75–80 cm and at the deepest point reached during sampling or at the encounter of the parent material. Some field measurements and analyses were performed in situ: texture, structure, and compactness (FAO, 2006), soil colour (Munsell soil colour chart, Munsell Color, 1994) and presence/traces of termite activity. The proportion of roots and the soil reaction to 10% HCl were described with indices from 1 (no root or no HCl reaction) to 4 (highest root density and reaction to acid). Twenty-eight holes were also drilled using an auger and core samples were tested in situ.

2.3. Physicochemical analyses

Sixty-five samples from sixteen distinct soils, representing the diversity observed in the field, were retained for laboratory analyses. The soil physicochemical proprieties included (i) particle-size distribution, assessed using a laser grain-sizer (Mastersizer 3000, Malvern Instruments), (ii) soil extraction using cobaltihexamine chloride to quantify the exchangeable cation and the Cation Exchange Capacity (CEC; Aran et al., 2008; Ciesielski et al., 1997; Orsini and Remy, 1976), (iii) pH_{H2O}, measured using a pH-meter (Orion Star A111, Thermo Scientific) after suspension in a 1:2.5 soil: water ratio, and finally (iv), OM content, analysed using Rock-Eval 6 pyrolysis (Technologie Vinci) of soil samples. Three parameters are measured during Rock Eval pyrolysis: (i) the Tmax (in °C), i.e. the temperature corresponding to the optimum hydrocarbon release during pyrolysis; (ii) the amount of pyrolyzed carbon in a N_2 atmosphere, or PC (Behar et al., 2001); (iii) the residual carbon, or RC, as the carbon content measured during the oxidation phase (Behar et al., 2001). In addition, the two indices proposed by Sebag et al. (2016) have been used, i.e. the I- index, emphasizing the degree of transformation of the immature organic fraction (related to SOM stabilization), and the R-index highlighting the contribution of the most refractory fraction or persistent SOM.

2.4. Soil micromorphology

Samples were taken for the making of thin sections used in soil micromorphology. Kubiëna boxes were utilized to sample the soil. The objective was to target some specific properties and features of soils (termite action, presence of charcoal, origin of the net transitions between horizons or layers, aspect of unidentified organic matter). Lastly, 15 Kubiëna boxes were sent for fabrication to Dr. Massimo Sbrana, *Servizi per la geologia* in Piombino, Italy. Thin sections were observed with an Olympus BX5 microscope coupled to an Olympus DP 72 digital camera. The terminology used to describe thin sections conforms to Stoops (2003).

2.5. Soil classification and mapping

Soils were classified following the World Reference Base for soil resources (IUSS Working Group WRB, 2014), based on field observations and laboratory analyses. As termites have a leading role in the soils from this area, a *Termitic* principal qualifier was used for soil presenting a hard carbonate termite-made horizon (compactness: hard or very hard; HCl reaction to carbonate: 3–4/4).

A soil map of the Chobe Enclave was produced using GIS tools (QGIS software 2.18.16), at a pixel resolution of 30 m × 30 m, based on the vegetation map of the Chobe Enclave and the positive correlation between the classification of the thirty-six soil profiles (grouped in five main groups: Chernozems-Phaeozems, Arenosols, salty/sodic soils, Kastanozems, and Calcisols) and their corresponding vegetation surveys (eight groups: Sandveld, *Baikiaea* forest, Dry floodplain grassland, *Colophospemum mopane* woodland, Mixed riverine forest, *Combretum hereroense* woodland, Dambo grassland and Wet floodplain grassland).

2.6. Data processing

Thermal stability of the OM was assessed using the I and R indices calculated from the pyrogram curves resulting from the Rock Eval pyrolysis (Sebag et al., 2016). The relationships between soil physicochemical parameters and soil diversity of the area were assessed using a principal component analysis (PCA) with eight physicochemical variables, i.e. Total Organic Carbon (TOC), I-index, R-index, exchangeable Ca^{2+}, Na^{+}, and K^{+}, CEC, and the sand percentage. PCA, correlations, and regressions between I and R indices were performed using MATLAB™ software (MATLAB R2016a, MathWorks Inc.).

3. Results

3.1. The Chobe Enclave's soil diversity

Based on the 36 soil profiles described in the field, seven different soil groups were identified according to the WRB (IUSS Working Group WRB, 2014): Arenosols (n = 13), Calcisols (n = 2), Chernozem (n = 1), Kastanozems (n = 12), Phaeozems (n = 4), Solonchak (n = 1), and Solonetz (n = 3). These soils are described in an Appendix document, data for each soil given in Appendix Table A.1, and their general properties are summarized in Table 1. The following section only focuses on the information related to their nature, specific locations, and/or associated vegetation patterns.

3.1.1. Arenosols

This is the main group of soils in the Chobe Enclave; they can be classified as *Arenic* as they contain a high proportion of sand (>70%). Despite this high sand proportion, *Arenic* soils are not systematically defined as Arenosols. Arenosols are mainly observed in two contrasted situations. Red sand areas are located on the southeastern side of the Chobe Fault, colonized by *Baikiaea plurijuga*/*Combretum elaeagnoides* forests and have their origin in extensive paleo wind-blown sand deposits elevated above the rest of the Chobe Enclave. White sand areas are more localized sandvelds (mainly as paleo river channels infilled by sands) with scattered to dense *Terminalia sericea* and/or *Philenoptera nelsii* stands or, in the north-east floodplains, covered by grasslands composed of *Aristida junciformis, Aristida meridionalis* and *Bulbostylis hispidula.*

Table 1

Physicochemical parameters of soils in the Chobe Enclave. Values are means of samples (n : number of samples) for each type of soil. Results marked with a star (*) refer to the mean of the various horizons of a single soil. CEC: cation exchange capacity [$cmol^{+}/kg$]; TOC: total organic carbon [%]; Clay, silt, sand: proportion of each particle-size [%].

	n	pH	Al^{3+}	Fe^{2+}	Mg^{2+}
Arenosols	20	6.5 ± 0.6	0.02 ± 0.05	0.01 ± 0.01	0.12 ± 0.06
Calcisols*	4	9.1 ± 0.7	0.01 ± 0.01	0.06 ± 0.01	0.63 ± 0.14
Chernozems*	4	8.9 ± 0.4	0.00 ± 0	0.29 ± 0.11	2.96 ± 0.47
Arenic Kastanozems	12	8.7 ± 0.6	0.00 ± 0	0.07 ± 0.02	0.62 ± 0.27
Siltic Kastanozems	12	8.3 ± 0.4	0.00 ± 0	0.13 ± 0.06	2.91 ± 1.60
Phaeozems*	4	6.8 ± 0.4	0.00 ± 0	0.23 ± 0.17	2.12 ± 1.61
Solonchaks*	4	10.1 ± 0.5	0.00 ± 0.01	0.19 ± 0.05	0.37 ± 0.45
Solonetz*	4	9.1 ± 1.9	0.01 ± 0.01	0.09 ± 0.05	0.37 ± 0.27
	n	Na^{+}	K^{+}	Ca^{2+}	CEC
Arenosols	20	0.00 ± 0	0.03 ± 0.03	0.64 ± 0.48	0.94 ± 0.63
Calcisols	4	0.68 ± 0.89	0.58 ± 0.17	3.44 ± 1.56	5.16 ± 1.56
Chernozems	4	0.08 ± 0.05	0.42 ± 0.24	16.58 ± 5.08	22.96 ± 9.49
Arenic Kastanozems	12	0.00 ± 0.00	0.26 ± 0.04	4.66 ± 1.19	6.04 ± 1.76
Siltic Kastanozems	12	0.11 ± 0.11	0.35 ± 0.28	10.40 ± 4.59	14.14 ± 6.31
Phaeozems	4	0.02 ± 0.05	0.25 ± 0.26	11.75 ± 9.69	17.61 ± 14.27
Solonchaks	4	13.93 ± 7.64	0.76 ± 0.25	1.53 ± 0.88	17.65 ± 5.39
Solonetz	4	5.02 ± 5.97	0.52 ± 0.47	1.19 ± 0.84	7.12 ± 5.51
	n	TOC	Clay	Silt	Sand
Arenosols	20	0.15 ± 0.13	0.8 ± 0.3	2.6 ± 1.7	96.6 ± 1.9
Calcisols	4	0.50 ± 0.25	7.0 ± 2.8	18.0 ± 4.3	75.0 ± 5.4
Chernozems	4	3.10 ± 1.62	11.7 ± 0.7	65.8 ± 2.4	22.5 ± 2.9
Arenic Kastanozems	12	0.47 ± 0.33	5.8 ± 1.2	25.9 ± 6.8	68.3 ± 7.3
Siltic Kastanozems	12	0.61 ± 0.41	15.2 ± 4.6	50.4 ± 12.0	34.4 ± 14.4
Phaeozems	4	2.44 ± 2.75	8.6 ± 5.5	42.9 ± 20.0	48.5 ± 25.3
Solonchaks	4	0.43 ± 0.16	13.3 ± 2.4	61.5 ± 4.3	25.2 ± 4.5
Solonetz	4	0.18 ± 0.14	7.5 ± 5.1	20.2 ± 6.1	72.3 ± 11.0

3.1.2. Kastanozems

Kastanozems are recognizable by their dark, organic, topsoil called *Mollic* horizon (dark-coloured surface horizon, with a high base saturation and >0.6% of soil organic carbon; IUSS Working Group WRB, 2014) and by a *protocalcic* or a *calcic* horizon, characterized by a HCl reaction ≥ 2/4. A common granular structure, sometimes changing to blocky/massive, is always clearly visible in the horizons (e.g. Fig. 2). These soil types are observed in different locations of the Chobe Enclave, but mostly on (i) carbonate (profile 1) and (ii) some diatomite deposits (profiles 30 and 31), situated in a landscape of islands and channels (Fig. 1). These areas are dominated by *Combretum hereroense* woodlands. However, Kastanozems are also found in sand-rich environments, where they are mostly characterized by a strong termite activity within their profile (profiles 10, 13, 14, 16, 20, and 27) and an increasing silt proportion with depth. These soils are often related to mixed riverine forests composed of various tree species such as *Philenoptera violacea, Berchemia discolor* or *Combretum mossambicense.*

3.1.3. Chernozems and Chernic Phaeozems

Chernozems and *Chernic* Phaeozems are soils with a high content of SOC and composed of a *Chernic* horizon (IUSS Working Group WRB, 2014). For most of them, they have a black topsoil horizon, which extends all along their profile (Fig. 2). The main difference between Chernozems and *Chernic* Phaeozems is that Chernozems include a *Protocalcic* or *Calcic* horizon while Phaeozems are devoid of carbonate. These soils are mainly located in depressions, such as channels where seasonal inundation by localized runoff occurs, forming dambos (Acres et al.,

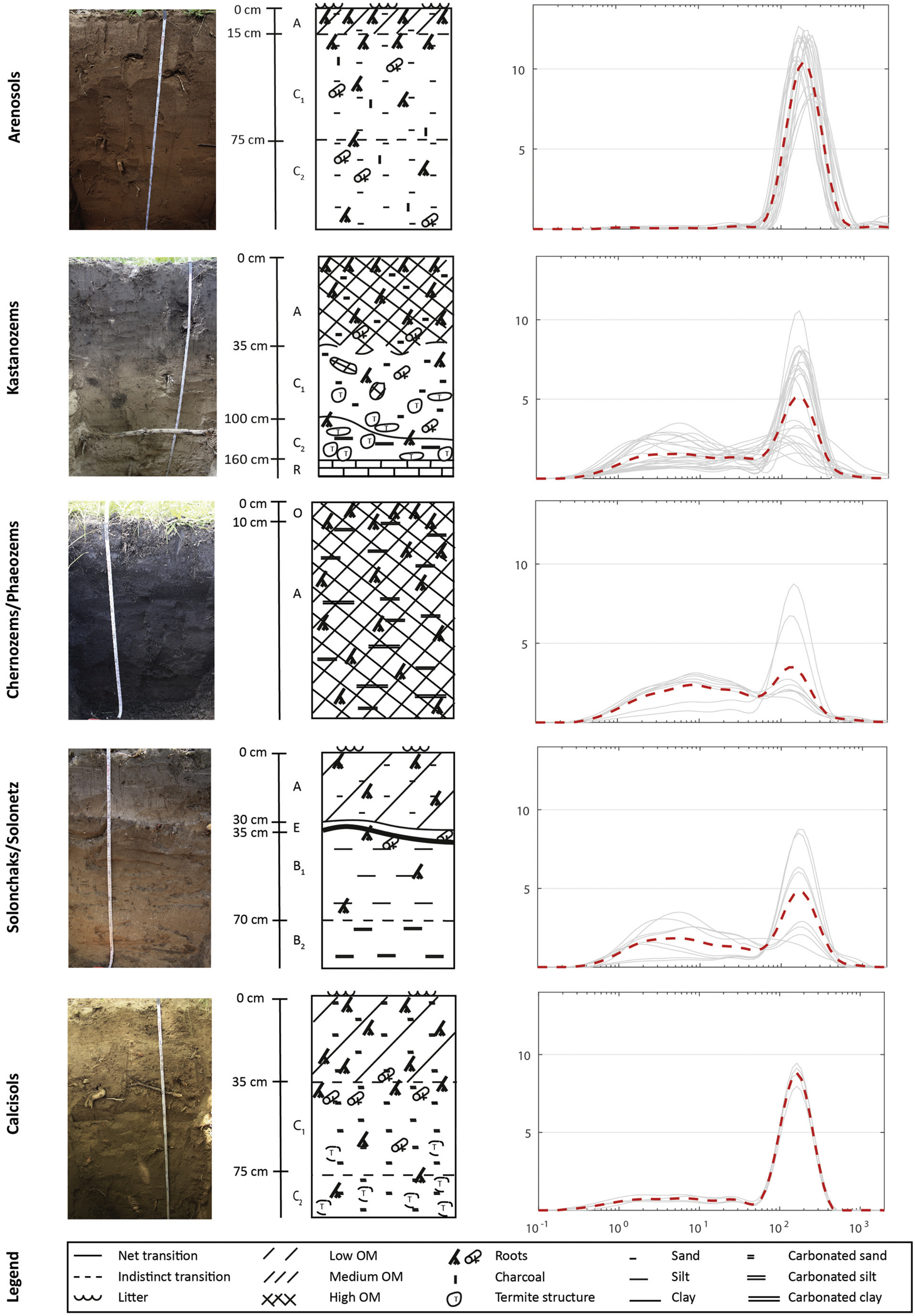

Fig. 2. Main soil types observed in the Chobe Enclave. A model soil was chosen for each soil type, described by a picture and an associated explanatory sketch. Numerous traces of termite structures are visible in these profiles, leading to the use of a new term, "*Termitic* horizon". Particle-size distributions are plotted with all measured samples for each soil type: x-axis corresponds to particle size [in μm] on a logarithmic scale and y-axis to frequency [in %]. The red dashed lines represent median distributions.

1985; Moore et al., 2007). They were always wet during the digging, but the water-table was reached only once (in profile 23). These areas are generally covered with dense and tall hydromorphic grasses, such as *Setaria sphacelata*, *Hyparrhenia rufa* or *Cimbopogon caesius*, which frequently burn during the dry season.

3.1.4. Solonchaks and Solonetz

Solonchaks and Solonetz are characterized by precipitation and accumulation of salts within their profile. They must contain a *Salic* or a *Natric* horizon, respectively (IUSS Working Group WRB, 2014). These salty and sodic soils were essentially covered by *Colophospermum mopane* woodlands. Some thin, sparse cryptogamic crusts were observed at the surface of Solonchaks and in several other locations of their area. Solonchaks and Solonetz were associated with stunted *Colophospermum mopane* woodland, where trees were likely undersized by the extremely high soil salinity and its associated effects on osmotic potential. However, tall mopane woodlands were also observed, but related with soils in which the horizons of high salinity were situated much deeper in the profile.

3.1.5. Calcisols

All observed Calcisols in the Chobe Enclave contain a *Calcic* horizon but without any *Argic* horizon above it (IUSS Working Group WRB, 2014). Carbonate layers, often observed in their lowest horizons, are interpreted as fossil palustrine limestones (Diaz et al., 2019), and therefore, are not of pedogenic origin. Calcisols are distinguished from Kastanozems by their low TOC concentration. One of them was around a termite mound, associated with palm trees (*Hyphaene petersiana* and *Phoenix reclinata*), the other one covered by *Colophospermum mopane* woodland.

3.2. The Chobe Enclave map of soils

Table 2 displays the relationships between the vegetation types and soils as correlation coefficients. All the stands of sandvelds and *Baikiaea* forests and the majority of dry floodplain grasslands are on Arenosols ($r = 1$). Similarly, the mixed riverine forests and *Combretum hereroense* woodlands are almost systematically associated with Kastanozems, and dambo grasslands with Chernozems or *Chernic* Phaeozems. They have been grouped in the soil map with the wet floodplain grasslands. It should be noted that no soil profile was dug in this last vegetation type; instead three core samples were taken with an auger in the north-east floodplains, revealing a black clayey soil. Soils are therefore probably Chernozems or *Chernic* Phaeozems, such as the ones observed in dambos. However, further studies need to be performed in order to check these results, particularly in the wettest areas, such as along the Linyanti River and in the depressions of the north-east floodplains.

Finally, *Colophospermum mopane* woodlands are largely observed on salty/sodic soils, i.e. 70% of their associated soils are Solonchaks, Solonetz or salty/sodic Arenosols (displaying high pH, generally >9). Some Solonetz are also found under *Combretum hereroense* woodlands, indicating a probable soil transition between the salty/sodic soils dominated by *Colophospermum mopane* and the Kastanozems on the carbonate/diatomite platforms supporting essentially *Combretum hereroense* woodlands.

Based on the resolution of the supervised vegetation map (i.e. 30 m), the proposed soil map (Fig. 3) displays a distribution of the various soil groups observed in the Chobe Enclave. It must be considered as a first approximation of the spatial distribution of the selected soil groups. Unfortunately, some soil groups, such as the localized Calcisol, cannot be represented on such a map due to its scale.

3.3. Soil organic matter (SOM)

Rock Eval parameters cannot be interpreted if samples contain a TOC < 0.2%. Therefore, some samples had to be excluded from this analysis. Too small a SOM concentration can potentially lead to miscalculations and bias in indices. Consequently, only 44 out of 65 soil samples were analysed using this method. Arenosols were thus poorly represented, as they have the lowest concentration in OM, and despite their large distribution in the Chobe Enclave.

The large majority of samples have a high Tmax peak, comprised between 400 and 470 °C. There are some exceptions, particularly in Solonchaks, where the Tmax is lower (Table A.1). The amounts of pyrolyzed carbon (PC) in the soils from the Chobe Enclave are small, generally five to fifteen times lower than the residual carbon (RC) proportion.

I and R indices (Fig. 4) cluster different sets of samples, and trends are organized by soil types. As expected (Sebag et al., 2016), there is no trend observable neither in the distribution of Arenosol samples nor in Calcisols (but the number of samples is limited); they have relatively homogeneous values of R-index (Table A.1). On the other hand, trends are observed in Kastanozem and Chernozem samples. Three of the four analysed Solonchak samples are characterized by high values of I-index, as well as samples from *Chernic* Phaeozems.

3.4. Multivariate analysis

The two first principal components (PC1 and PC2) explain 43.5% and 31.2% of the total variance of the samples, respectively (Fig. 5). The circle of correlations shows that all the variables are positioned between two circles, meaning that they are all significant and well correlated to the two principal components ($r > 0.8$). PC1 stretches between two poles, almost perfectly opposed, one composed by exchangeable Ca^{2+}, TOC and the CEC, and the other by sand percentage. On the PC2 axis, R and I indices are opposed, with Na^{+} close to I-index, and almost perpendicularly to the PC1 axis, meaning that these variables are independent of the previously mentioned variables.

According to this PCA, Arenosol samples are very similar to Calcisol samples, whereas Kastanozem, Chernozem, *Chernic* Phaeozem and Solonchak samples are more heterogeneous, scattering across large ranges along PCA1 or PCA2.

4. Discussion

The region of the Chobe Enclave is characterized by a high diversity in soils, despite being located in the continuous sand body of the Kalahari (Wang et al., 2007). The proposed soil map (Fig. 3) clearly emphasizes a much higher diversity than expected, also with some discrepancies in soil categories and distributions compared with previous maps (Remmelzwaal and Van Waveren, 1988; De Wit and Nachtergaele, 1990; European Soil Data Center (ESDAC), 2014). However, the survey was performed at a different scale of details in these previous studies. The recent vegetation map from Sianga and Fynn (2017) suggests this underlying diversity as well. Possible explanations for such a soil diversity are discussed in the following sections. The proposed arguments are based on two main subjects: (i) historical landscape dynamics, which influenced surficial geology, topography, and hydrology, and (ii) biological factors, related to termites and plants, and their residues after fires.

4.1. The roles of surficial geology, topography, and hydrology

The type of sands, on which soils developed, has limited influence on their characteristics, because of the similar soil physicochemical characteristics, which is emphasized by their closeness in the principal component analysis plot (Fig. 5). However, the specific phase associated with exchangeable Al^{3+}, detected in low amounts in red sand Arenosols, is mostly expressed as coatings on quartz grains (their chitonic related distribution; Fig. 6.1); it is this Al^{3+}-phase that is partly responsible for the soil low pH, as the Al^{3+}-phase is known to be one of the main compounds responsible for soil acidity (Thomas

Table 2
Distribution of soil types among the vegetation types in the Chobe Enclave; n : number of soil investigated (49 in total: 32 soil profiles and 17 auger cores) associated with each vegetation type. The different shades of grey correspond to the strength of the correlation between the vegetation types and soils (0–0.25 = dark grey, 0.25–0.75 = light grey, 0.75–1 = white). Only two profiles were dug in the *Baikiaea* forests; however, there is much evidence of the close affinity between the latter and Arenosols (McCarthy et al., 2005; Sianga and Fynn, 2017).

	n	Chernozem/*Chernic* Phaeozem	Kastanozems	Calcisols	Solonchak/ Solonetz	Arenosols
Sandveld	7	0	0	0	0	1
Dry floodplain grassland	5	0	0.2	0	0	0.8
Baikiaea forest	2	0	0	0	0	1
C. mopane woodland	10	0	0	0.1	0.7	0.2
Dambo grassland	7	1	0	0	0	0
C. hereroense woodland	8	0	0.875	0	0.125	0
Mixed riverine forest	7	0	1	0	0	0
Wet floodplain grassland	3	1	0	0	0	0

and Hargrove, 1984; Table A.1). They support different and distinct vegetation communities: red sands Arenosols are covered by *Baikiaea* forests (McCarthy et al., 2005; Sianga and Fynn, 2017), and white sands by grasslands and *Terminalia sericea*/*Philenoptera nelsii* sandvelds. Their respective topographic positions are a possible explanation for the distribution of Al/Fe coatings of these sands. Indeed, red sand Arenosols are located in elevated areas, along the Chobe Fault (up to 40 m higher than the floodplain), in the horst side of the system. They were probably deposited and/or reworked by winds (they are extremely well sorted with very leptokurtic curves; Fig. 2), without any significant contact with running water, and therefore, able to preserve their Al/Fe coatings that give the reddish colour. Conversely, the white sands from channels were transported by water, which probably contributed to remove sand coatings and to clean their surface.

Although all the soils of the area are widely impacted by the presence of sands, Arenosols are characterized by a relatively low R-index compared to the other soils (Fig. 4), except Phaeozems and Solonchaks. It means that their organic matter has a low thermal stability compared to other soils. This can be explained by their lack of mineral preservation of OM due to their almost exclusively sand fraction composition; indeed, clays are known to be efficient in SOM preservation (Lehmann and Kleber, 2015), a process referred to as their "shield effect". This lack of OM preservation, associated with a low TOC in Arenosols of the Chobe Enclave, suggests an easy access to, and a rapid turnover, of OC in sandy soils, i.e. large proportions of the carbon pools are mainly contained in flora in these ecosystems, not in soils. In addition, these

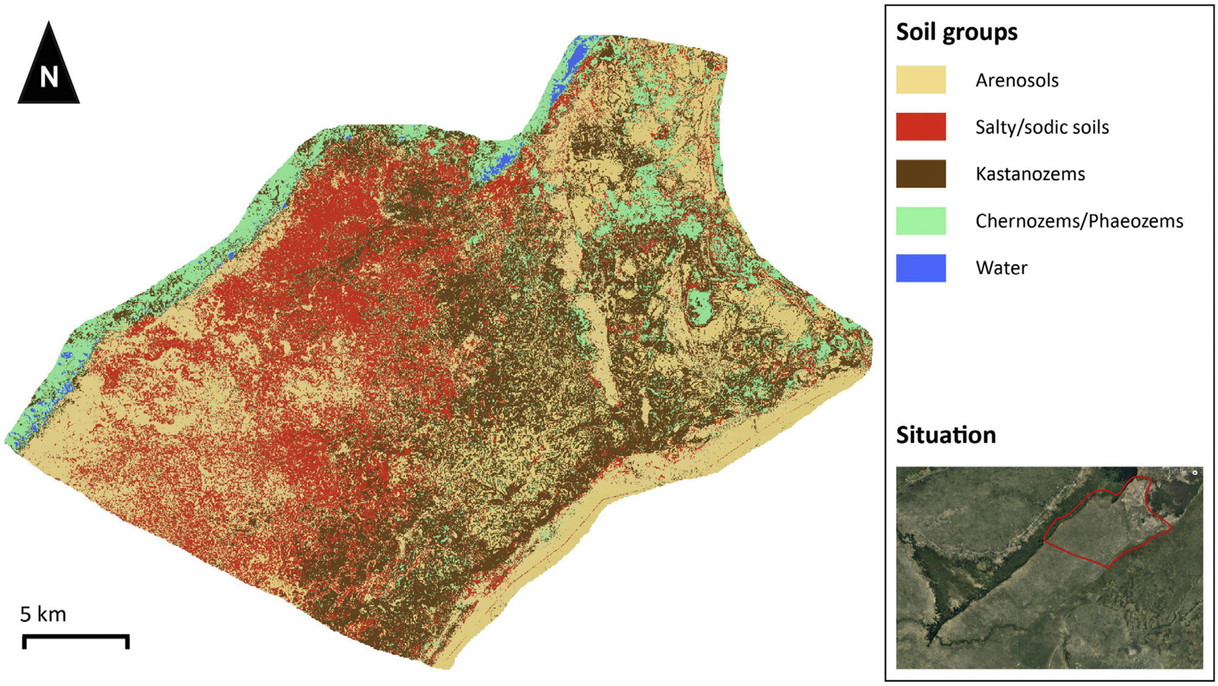

Fig. 3. Soil map of the north-eastern part of the Chobe Enclave. No soil profile was described under the permanent water areas and the north-eastern wet floodplains soils were only sampled using an auger.

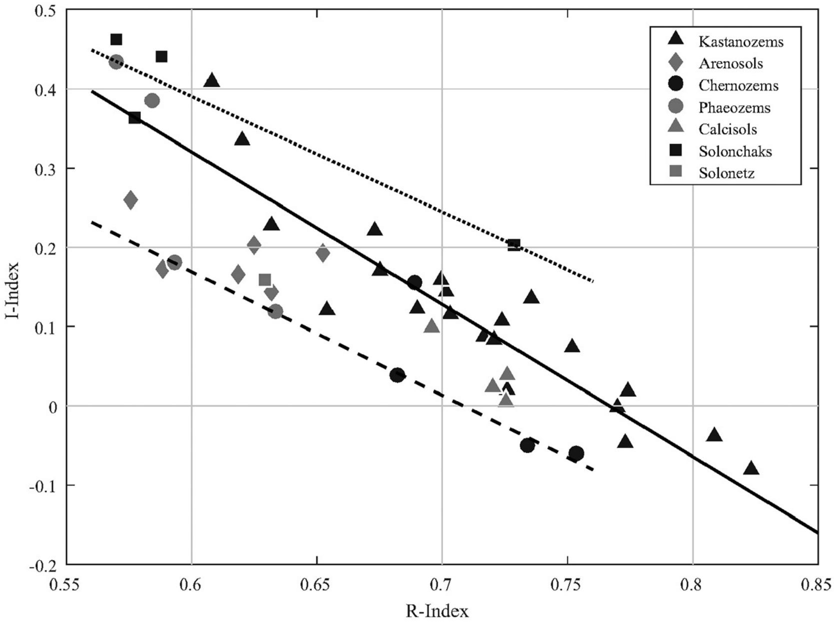

Fig. 4. Plot of I- vs R-indices according to soil types. Best fit regression lines are added for Solonchak (dotted line), Kastanozems and Calcisols (continuous line), and *Chernic* horizons (Chernozems and Phaeozems; dashed line).

samples do not follow a linear trend on the I/R plot (Fig. 4). This observation corresponds to previous analyses made on other Arenosols samples worldwide, notably in Niger and northern Cameroon (Sebag et al., 2016). Indeed, in Arenosols, the efficient mineralization of OM due to a large and easy access to it (i.e. labile and/or resistant but accessible pools), results in a relative decrease of the refractory pool, shifting the R-index towards low values.

Soil thin sections of ancient palustrine/lacustrine deposits emphasize a combination of phytoliths, diatoms, and amorphous silica (Fig. 6.2). The abundance of the latter indicates an important recycling of the amorphous diatomitic source, as commonly observed in the semi-arid zone (Sebag et al., 1999). Soils found on these beds are mainly *Siltic* Kastanozems. Their fine particle-size distribution essentially originates from their parent material (carbonate and diatomite), but also from

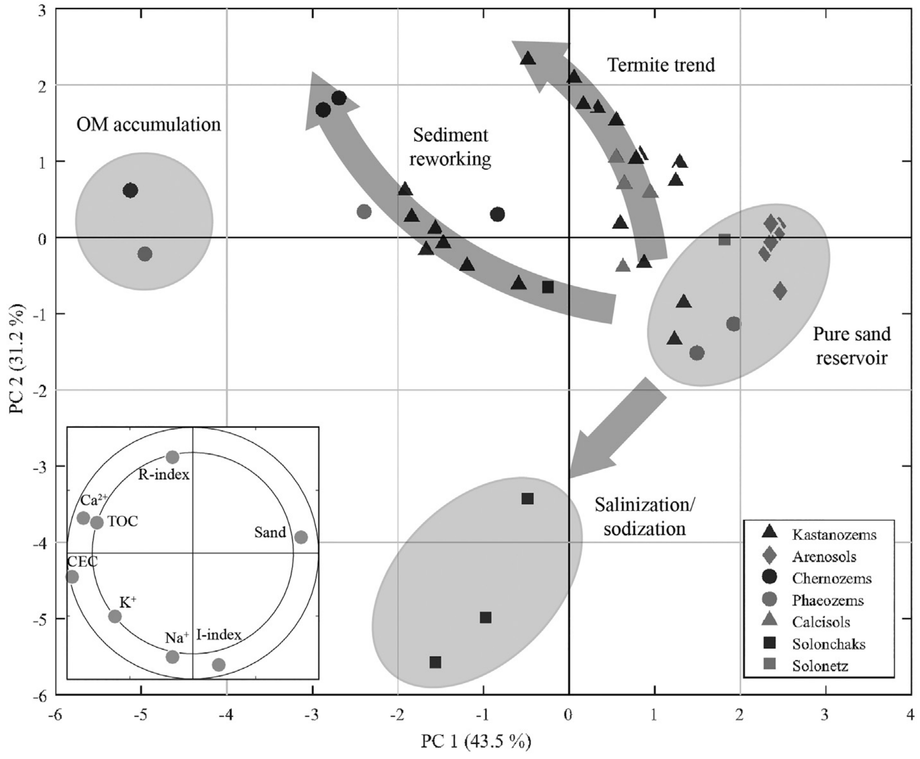

Fig. 5. Projection of soil types on the principal component 1 (PC1) x principal component 2 (PC2) plane. Percentages in the legend axes refer to the proportion of explained variance. Lower-left corner: circle of correlation coefficients between the eight variables used in the PCA and the first and second principal components. The circle has a radius of 1 (i.e. r = 1), the centre of the cross being at 0. The inner circle has a radius of 0.8 (i.e. r = 0.8). The grey arrows and the light grey round areas display respectively (i) the different trends and their associated processes and (ii) some specific soil settings. OM: organic matter. "Sediment reworking" refers to the mobilization of alluvial deposits and aeolian dust input.

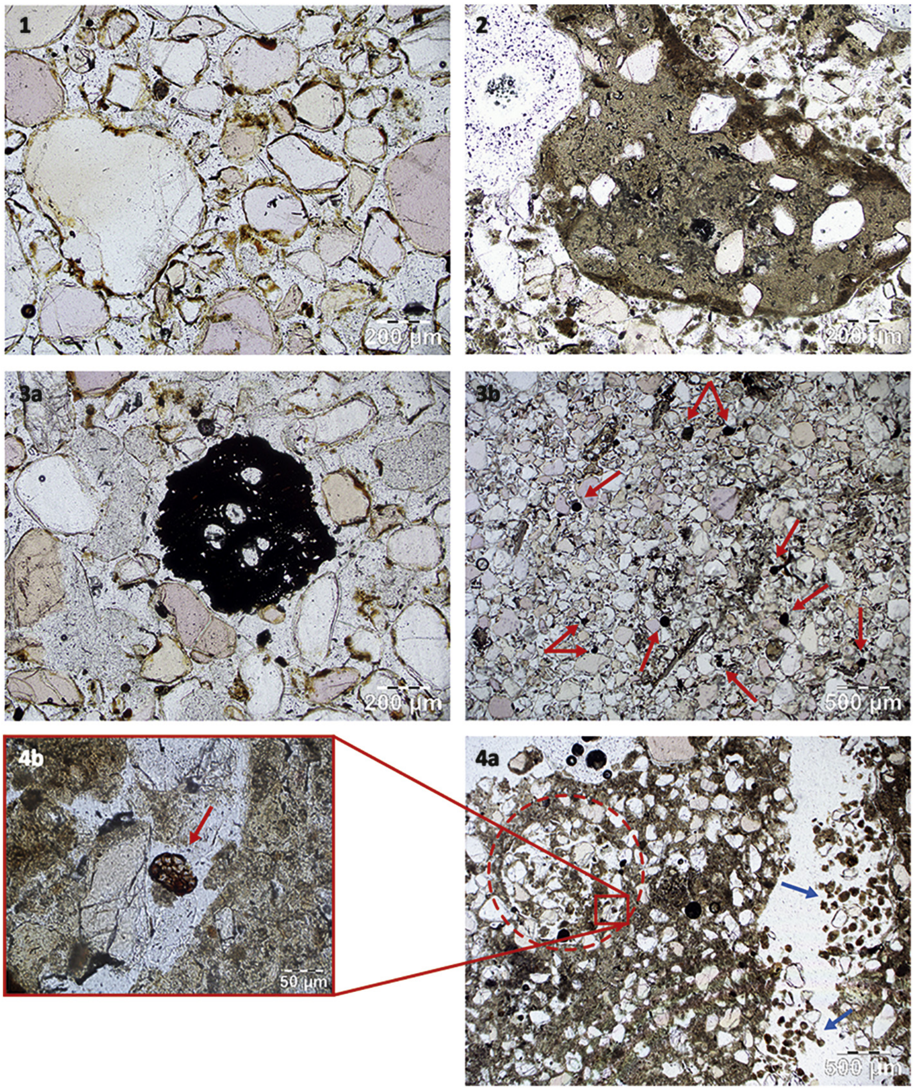

Fig. 6. 1) Chitonic c/f related distribution with Fe—Al oxyhydroxide coatings around quartz grains in a red sand Arenosol from the Chobe Enclave (Profile 8). The grain-size distribution of quartz grains is well sorted, and the voids result from the loose packing of the soil components (simple packing voids). **2)** Silicification of soil particles (the two shades of brown of the central particle; profile 14). The high availability of amorphous silica originating from diatomite beds is an important source of silicification. **3a)** Big charcoal particle (profile 8). **3b)** Multiple carbon beads (red arrows) in a sandy matrix (profile 12). **4a)** Thin section of a *Termitic* horizon (profile 13), with the presence of multiple termite pellets (blue arrows) and an infilled termite tunnel (inside the red dashed circle). **4b)** Inside the termite tunnel was found a spore, possibly from *Termitomyces sp* (red arrow).

airborne dust trapped by the vegetation and incorporated into soils, as observed in the Okavango Delta (Humphries and McCarthy, 2014). Weathering of the carbonate bedrock also results in high quantities of exchangeable Ca^{2+} in these soils (Table 1). Their relatively high CEC and OM content are probably due to the combined effect of clays and Ca^{2+}, an ion known to stabilize OM (Stockmann et al., 2013; Rowley et al., 2018). This effect is similarly observed in all the Ca^{2+}-rich soils (Kastanozems and Calcisols mainly), whose OM follows the same trend on the I/R diagram (Fig. 4), with high R values corresponding to thermally stable OM.

The central area of the Chobe Enclave is occupied by a system of islands and channels, resulting in a complex microtopography (see section “Study site” in Materials and Methods). Carbonate and diatomite beds forming the islands are separated by fossil alluvial channels, with sandvelds (as discussed above), or humid depressions infilled with fine alluvium. The most humid areas, i.e. dambos (Moore et al., 2007), are characterized by a high water-table, or a permanent water body, a few months during the year. The Chernozems and Phaeozems, developed in these areas, include the highest proportions of clays and SOC of the Enclave (Table 1). SOM accumulation is probably partly due to the presence of waterlogging, which regularly creates anoxic conditions during heavy rainfalls or floods, added to a high clay and silt content, probably transported and accumulated in these depressions by water runoff from the multiple islands rich in fine particles. Moreover, savannah fires frequently hit these parts of the landscape, and fire residues can also contribute to SOM accumulation (see *Charcoal and plants* section). The macrofauna likely also plays a role in SOM accumulation, as they are attracted by these dambo grasslands during the wet season (young, nutrient rich grass) as well as during the dry season (presence of green forage; Fynn et al., 2014; Sianga and Fynn, 2017). While grazing, they generate consequent quantities of faeces, which are known to enrich both soil CEC and OM content (McNaughton et al., 1997; Skarpe et al., 2004). Moreover, by rolling themselves in waterholes, elephants remove large quantities of mud and enlarge the depressions (Haynes, 2012), attracting more animals, which further fertilize the soils with their faeces (positive feedbacks). These specific locations allow such tropical Chernozems and *Chernic* Phaeozems to develop in these unexpected settings, whereas they are mostly found under steppes, grasslands, or pampas (IUSS Working Group WRB, 2014; Ryan, 2014).

The topography of the Chobe Enclave, at a larger scale, has an impact on the soil diversity as well. Indeed, the low gradients of elevation from the Chobe Fault to the Linyanti (~8 m for 25 km) and from the NE to the SW (~10 m for 50 km) are sufficient to induce a drought gradient, particularly visible in the direction of the SW, where neither river nor running water reaches the areas. Kastanozems and their associated *Combretum hereroense* woodlands (in brown on the map; Fig. 3) are gradually replaced by salty/sodic soils (mainly Solonchaks, Solonetz and salty Arenosols; in red on Fig. 3), covered by *C. mopane* woodlands. The presently dry conditions of these areas do not necessary lead to an accumulation of Na^+ (a sufficient source of Na^+ is lacking). These deposits were probably formed during wetter conditions than today by the same evapotranspiration mechanism as described by McCarthy and Humphries in the islands of the Okavango Delta (McCarthy et al., 2012; Humphries and McCarthy, 2014). Therefore, the high concentrations of Na^+ in these soils are probably derived from ancient salt deposits, the parent material of Solonetz and Solonchaks being interpreted as sodic paleosols. However, the unexpected stability of Na^+ remains a challenge in a region where the rainfall still reaches 650 mm per year (Jones, 2002; Burgess, 2006). A possible explanation can be a specific property of such soils, i.e. the reduction of its permeability (the "osmotic explosion effect" associated to high Na^+ adsorption on clays; Amezketa and Aragües, 1995; Legros, 2007), consistent with the high compacity of these soils observed in situ. The soil chemistry, dominated by Na^+, influences the SOM as well. First, a salt accumulation leads to a lower SOC content (Wong et al., 2010), as observed in the Enclave despite high contents in clays and silts (Table 1, Fig. 2). Second, Na^+ has a high impact on SOM dynamics, as shown by a "sodic trend" in the I/R plot (dotted fit-line, Fig. 4), with a relatively higher I-index compared to the other soils, meaning a higher proportion of thermally immature OM (Sebag et al., 2016). This trend is attributed to a substantial decrease of microbial and enzymatic activities with increasing salinity (Yuan et al., 2007). Also of interest, is the patchy nature of these Solonchaks, as demonstrated by the highly patchy nature of stunted and tall mopane woodlands with stunted mopane being associated with the Solonchaks. It is not clear what mechanism gave rise to the patchy nature of these salt deposits. These Solonchaks may play a key role in providing Na and other mineral elements to herbivores, critical for reproduction and lactation (Fynn et al., 2014).

4.2. Termites

As mentioned above, a large part of the soils in the Chobe Enclave is developed on sands. However, relatively high proportions of silts and clays were found in soils developed on the widespread sandy material. Aside from possible contributions of alluvium and aeolian particles, termites are likely responsible for fine particle-size distributions, as they are omnipresent in the area; their hard-built structures were found associated to 6 of the 36 soil profiles. Their effect on soils is illustrated on the PCA plot (Fig. 5). In sandy areas, they are at the origin of the transformation of Arenosols into *Arenic* Kastanozems, and possibly, Calcisols. Indeed, termites are known to have a large impact on physicochemical proprieties of soils, by increasing their proportion of silt and clay, modifying the soil structure, and by increasing their cation concentrations and pH (McCarthy et al., 1998; Jouquet et al., 2007, 2011; Menichetti et al., 2014; Muvengwi et al., 2016). It has been demonstrated by Jouquet et al. (2007) that they are able to transport clays from deep soil horizons to the surface and use it to cover their exosymbiotic fungus comb. In the north-east floodplains, under the influence of termites, proportions of silt and clay increase from <3% in Arenosols (e.g. profile 34) to >30% in a Calcisol found on a "termite island" (e.g. profile 33, 20 m away from profile 34). This fine grain-size proportion is higher than those observed in previous studies in the Okavango delta, where clay contents close to the termite mounds were only twice as high than in the surrounding soils (McCarthy et al., 1998). Furthermore, the relative proportion of K^+ vs the concentration of other exchangeable cations was higher in the Calcisol than any other soil of this study. This can be explained by the fact that termites modify clay proprieties in their nest by creating smectite layers from initial material such as illite. They do so by removing potassium and releasing it in the outer solution using either their saliva or by stimulating microflora with their saliva in the litter (Jouquet et al., 2007).

Moreover, termites have an indirect impact on SOM. Indeed, on a small transect, concentrations of SOC rose from almost absent (0.01–0.07%; profile 34) to values close to 1% (0.25–0.81%; profile 33). As discussed above, TOC in sandy soils is very low; consequently, an increase in fine grain-size particles and cations leads to a proportional increase of TOC (Blanchard et al., 2005; Lehmann and Kleber, 2015). In addition, the presence of calcium carbonate, and associated exchangeable Ca^{2+} measured in sandy soils influenced by termites, also contributes to SOM dynamics (Rowley et al., 2018), as demonstrated by the clustering of these soils with *Siltic* Kastanozems on the I/ R plot, displaying a "*Calcium trend*" (continuous fit-line, Fig. 4). Termites also directly influence SOM, firstly, and particularly in sandy soils, as they enhance the SOM content by bringing faeces and by using their saliva to build and stabilize their nest (Fig. 6.4a, Jouquet et al., 2002, 2007). Secondly, they increase litter decomposition rates (Gutteridge and Reumerman, 2011; Menichetti et al., 2014), and are probably partially responsible for the absence of litter at the surface of soils in the Chobe Enclave. Indeed, 14 of the 36 profiles analysed were totally deprived of litter, and the other ones were only patchily covered. Depending on the local conditions and the available resources, termites can consume up to 90% of the herbaceous biomass (Mugerwa et al., 2011). They substantially increase the incorporation of OC in soils. This input of fresh OM in soils can be observed when residual (RC) and pyrolysed carbon (PC) are compared (Fig. 7). All the soil samples taken in *Termitic* horizons were identified and marked in black. They belong to soils from various areas of the Chobe Enclave, developed on different surficial geological sediments. But they follow the same linear trend, with a similar RC/PC ratio, lower from the other samples not affected by termites. This ratio indicates a higher proportion of PC, and thus a lower proportion of RC after pyrolysis. This also means that the large proportion, if not all, of the SOC in these samples was added or transformed by termites.

By all their actions, termites fertilize poor sandy soils by improving their texture, their structure, and the stabilization of carbon. They create islands of dense vegetation in poor sandy areas, because of the more fertile soils and the conditions less subject to negative feedback from water variations (Corrennblit et al., 2016). These islands support a specific type of vegetation, absent in the surrounding areas, such as palm trees (*Hyphaene petersiana*, *Phoenix reclinata*). Termites have already been recognized as the source of the mosaic landscapes observed in savannahs (Jouquet et al., 2011), and the accumulation of nutrients through termite activity forms nutrient hot-spots for improved forage nutritional value for herbivores (Grant and Scholes, 2006).

4.3. Charcoal and plants

The relationships between plants and soils are complex in the Chobe Enclave. For instance, *Combretum imberbe* has a probable direct impact on soils through the oxalate-carbonate pathway, previously observed under Iroko trees (*Milicia excelsa*) in central Ivory Coast (Cailleau et al., 2004), *Pentaplaris davidsmithii* and *Ceiba speciosa* in South America (Cailleau et al., 2014), *Brosimum alicastrum* in Haïti (Rowley et al., 2017). This phenomenon, first observed in a calcrete in Israel (Verrecchia, 1990), is due to oxalotrophic bacteria using calcium oxalate ($Ca(COO)_2$) in their metabolism, leading to an alkalinisation of the soil environment, and potentially to calcium carbonate precipitation when a favourable pH is reached (Verrecchia et al., 2006). This was identified in one soil (profile 9), close to *Combretum imberbe,* where, despite the deep sandy substratum on which the soil is developed, and the absence of termites, reactions to HCl reached 2/4 with a pH $= 8$, indicating a

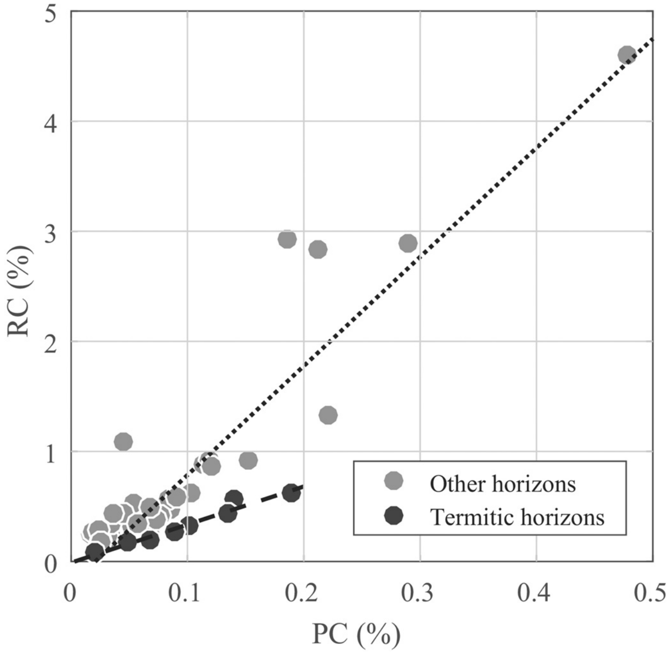

Fig. 7. Residual Carbon vs Pyrolized Carbon diagram according to the presence (black dots) or absence (grey dots) of termite structures in the sampled horizons. Two fitting lines are added to emphasize the different trends in the RC/PC ratios.

clear alkalinisation and the presence of calcium carbonate, probably related to the oxalate-carbonate pathway.

The majority of the soils were not covered by litter, as already mentioned, and whenever litter was present, it was fresh plant debris from the year. This indicates a fast decomposition or integration into soils of the plant litter, partly by termites as discussed above, but also by combustion due to fires during the dry season. Numerous marks of savannah fires have been observed in the whole Chobe Enclave, especially in dambos, where the majority of the surfaces burns each year. Although it is a natural factor of such dry tropical areas, their frequency is strongly enhanced in the Chobe Enclave by inhabitants. Fire residues are observed in soils, as for example black carbon (BC) and charcoal particles (Fig. 6.3a, b). It has been shown that fire residues can compose up to 35% of the SOM in some grasslands (USA) and even 60% in Chernozems (Canada; Preston and Schmidt, 2006). Fire-derived OM has a major impact on SOM, illustrated in general by high Tmax peaks (Table A.1) corresponding to the pyrolysis of pedogenic transformed and refractory OM (Sebag et al., 2016). In the case of Chernozems and Phaeozems under dambos, the I/R ratio is higher than in the other soils, as shown by the dashed regression line on the I/R plot (Fig. 4); this indicates an even higher proportion of refractory OM. This is probably the consequence of a high content in clays combined with a high content in BC, phyllosilicates being known to protect some refractory SOM (Lehmann and Kleber, 2015; Sebag et al., 2016). A dense fine root system was also observed in these soils, originating from grasses covering these areas, such as *Setaria sphacelata* or *Hyparrhenia rufa*. These observations correspond to the recent conclusions about SOM dynamics, which emphasizes the role of root- as well as fire-derived carbon as sources of SOC in some specific soils (Rasse et al., 2005; Schmidt et al., 2011; Lehmann and Kleber, 2015).

5. Conclusion

This study of soils from the Chobe Enclave highlighted the important diversity of them in what is considered as an apparently homogeneous sandy area, previously mapped as mostly covered by Arenosols. The large number of in situ observations, as well as laboratory and data processing, emphasize the fact that this soil diversity results from the interaction between multiple factors. The deep sandy deposits, originating from past drier climates, constitute the main factor of development of white- and red-sand Arenosols, depending on their reworking or not by water. Hydrological settings also play a major role in the development of Chernozems and Phaeozems, by concentrating alluvium and creating anoxic conditions, leading to the preservation of soil organic matter to some extent. A vast island system was also found in the central part of the Enclave, formed by carbonate and diatomite beds, leading to moderately-rich organic soils, such as Kastanozems. On some islands, both high concentrations of Na^+ and high pH (up to 11.3) indicate a strong influence of salts and the development of Solonetz and Solonchaks. The significant presence of termites in the area strongly shapes the topography and leads to major transformation of the soil chemistry and structure. Finally, black carbon undoubtedly plays an essential role in SOM dynamics of the region as demonstrated by the high quantities of refractory OM measured by Rock Eval pyrolysis, the numerous traces of fires observed in situ, and the presence of charcoal particles in soil thin sections. These various soil patterns play an important role in creating functional habitat heterogeneity for promoting adaptive foraging options for herbivores (Fynn et al., 2014). Thus, this soil study has contributed to a greater understanding of herbivore ecology in the region, with associated conservation implications.

This research was a first assessment to explore, survey and map the soil diversity of the Chobe Enclave; it provided not only a better understanding of the soil dynamics, but also brought new observations regarding the surficial geology and geomorphology of the area. However, further research is needed to identify the origin of the multiple sedimentary deposits, such as the diatomite and carbonate beds, as well as, in the north-eastern wet floodplains, the origin of grasslands where no soil profile could be dug.

Acknowledgements

We express our sincere thanks to the Ministry of Environment, Natural resources conservation and Tourism of the Republic of Botswana as well as the Chobe Enclave Conservation Trust for the research permits, without which this study would not have been possible. The authors also warmly thank Dr. Nathalie Diaz for her advises, Mike Rowley, Laetitia Monbaron, Micaela Faria, and Thierry Adatte, who contributed to laboratory analyses, and the entire staff and the director of the Van Thuyne-Ridge Research Centre, who provided the perfect environment for research conditions. We are also grateful to Karin Verrecchia who kindly edited the first version of the manuscript. We finally like to thank two anonymous reviewers and the Editor-in-Chief Prof. Hartemink for their improving and constructive remarks on the manuscript. This work has been partly supported by a Swiss National Foundation grant no 200021_172944 to Eric P. Verrecchia.

Appendix A

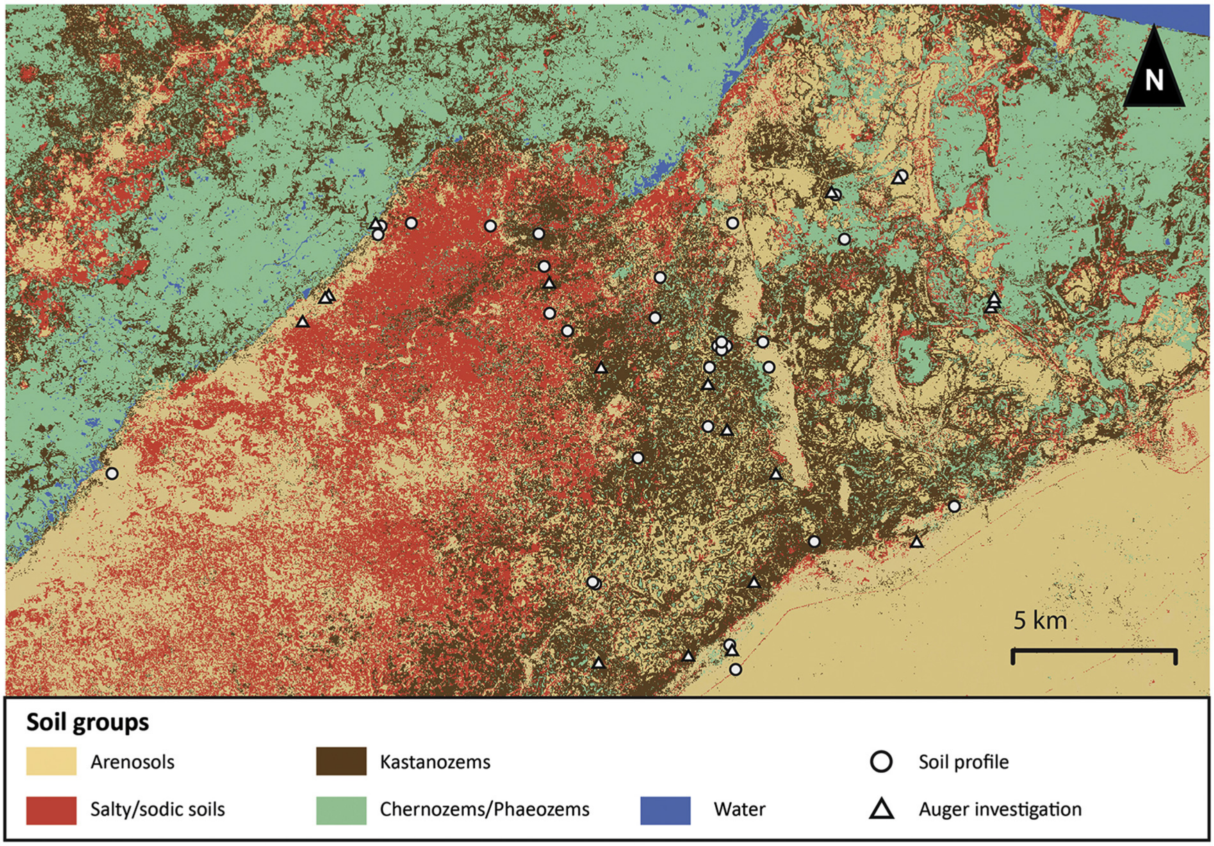

Fig. A.1. Distribution of the observed and/or sampled soils in the Chobe Enclave.

Table A.1
Data from the observed profiles (by their number) in the Chobe Enclave.

Profile number	Soil group (WRB)	Depth (cm)	Al^{3+} (cmol + kg^{-1})	Fe$^{2+/3+}$ (cmol + kg^{-1})	Mg^{2+} (cmol + kg^{-1})	Na^{+} (cmol + kg^{-1})	K^{+} (cmol + kg^{-1})	Ca^{2+} (cmol + kg^{-1})	CEC (cmol + kg^{-1})	Clay (%)	Silt (%)	Sand (%)
1	Kastanozem	15	0.00	0.15	3.28	0.12	0.61	13.99	17.02	14.16	57.29	28.55
		30	0.00	0.15	3.59	0.08	0.67	13.15	18.06	18.17	61.38	20.46
		50	0.00	0.08	1.42	0.07	0.64	9.61	11.39	9.46	54.40	36.15
		80	0.00	0.19	4.26	0.23	0.76	11.17	21.73	6.93	36.87	56.20
8	Arenosol	15	0.18	0.00	0.07	0.00	0.07	0.21	0.69	1.25	3.43	95.32
		30	0.13	0.00	0.11	0.00	0.08	0.33	1.05	0.84	3.19	95.97
		50	0.03	0.01	0.16	0.00	0.06	0.64	1.04	0.93	2.55	96.51
		80	0.01	0.00	0.18	0.00	0.08	0.85	0.64	1.42	4.77	93.81
12	Arenosol	15	0.00	0.01	0.26	0.00	0.06	0.98	1.37	1.12	7.19	91.69
		30	0.00	0.01	0.17	0.00	0.05	0.69	1.09	0.86	2.93	96.21
		50	0.00	0.00	0.10	0.00	0.04	0.45	−0.08	0.57	0.49	98.94
		80	0.00	0.00	0.10	0.00	0.03	0.35	0.32	0.54	0.42	99.04
13	Kastanozem	15	0.00	0.08	2.56	0.02	0.11	5.25	8.74	16.67	57.39	25.94
		30	0.00	0.07	2.03	0.07	0.05	4.71	7.32	22.97	42.78	34.24
		50	0.01	0.07	0.58	0.06	0.02	6.18	6.86	15.00	44.37	40.63
		80	0.00	0.06	0.49	0.07	0.01	4.52	4.70	10.63	21.69	67.68

Profile number	Soil group (WRB)	pH	RM (%)	TOC (%)	HI (mg HC/g TOC)	OI mg CO2/g TOC)	PC (%)	RC (%)	Tmax (°C)	R-index A3 + A4/100	I-index log [(A1 + A2)/A3]
1	Kastanozem	8.7	2.32	0.56	96.34	261.33	0.09	0.48	412	0.703	0.116
		8.8	3.32	0.31	122.28	409.71	0.07	0.24	415	0.701	0.145
		8.7	1.18	0.23	122.75	355.65	0.05	0.18	414	0.673	0.221
		9.2	3.28	0.23	96.86	362.15	0.04	0.19	420	0.699	0.159
8	Arenosol	5.7	0.03	0.26	87.80	197.87	0.03	0.23	416	0.632	0.144
		6.0	0.04	0.16	63.91	216.03	0.02	0.14	406	0.596	0.33

Table A.1 (*continued*)

Profile number	Soil group (WRB)	pH	RM	TOC	HI	OI	PC	RC	Tmax	R-index	I-index
			(%)	(%)	(mg HC/g TOC)	mg CO2/g TOC)	(%)	(%)	(°C)	A3 + A4/100	log [(A1 + A2)/A3]
		5.9	0.03	0.14	58.72	281.20	0.02	0.12	411	0.601	0.316
		6.8	0.04	0.12	77.08	270.20	0.02	0.10	412	0.607	0.314
12	Arenosol	6.9	0.03	0.26	84.79	221.46	0.03	0.23	406	0.576	0.26
		7.1	0.03	0.17	59.56	194.60	0.02	0.15	339	0.59	0.345
		7.0	0.01	0.01	316.75	1338.37	0.01	0.00	326	0.584	0.464
		6.9	0.01	0.05	76.96	289.67	0.01	0.05	313	0.565	0.485
13	Kastanozem	7.8	0.72	1.55	123.30	145.12	0.22	1.33	446	0.823	−0.08
		7.9	0.75	1.07	116.96	164.43	0.15	0.92	446	0.809	−0.038
		8.6	0.79	0.70	156.06	250.51	0.14	0.56	461	0.774	0.018
		9.0	0.74	0.43	168.35	335.29	0.10	0.33	466	0.735	0.135

Profile number	Soil group (WRB)	pH	RM	TOC	HI	OI	PC	RC	Tmax	R-index	I-index
			(%)	(%)	(mg HC/g TOC)	(mg CO2/g TOC)	(%)	(%)	(°C)	A3 + A4/100	log [(A1 + A2)/A3]
1	Kastanozem	8.7	2.32	0.56	96.34	261.33	0.09	0.48	412	0.703	0.116
		8.8	3.32	0.31	122.28	409.71	0.07	0.24	415	0.701	0.145
		8.7	1.18	0.23	122.75	355.65	0.05	0.18	414	0.673	0.221
		9.2	3.28	0.23	96.86	362.15	0.04	0.19	420	0.699	0.159
8	Arenosol	5.7	0.03	0.26	87.80	197.87	0.03	0.23	416	0.632	0.144
		6.0	0.04	0.16	63.91	216.03	0.02	0.14	406	0.596	0.33
		5.9	0.03	0.14	58.72	281.20	0.02	0.12	411	0.601	0.316
		6.8	0.04	0.12	77.08	270.20	0.02	0.10	412	0.607	0.314
12	Arenosol	6.9	0.03	0.26	84.79	221.46	0.03	0.23	406	0.576	0.26
		7.1	0.03	0.17	59.56	194.60	0.02	0.15	339	0.59	0.345
		7.0	0.01	0.01	316.75	1338.37	0.01	0.00	326	0.584	0.464
		6.9	0.01	0.05	76.96	289.67	0.01	0.05	313	0.565	0.485
13	Kastanozem	7.8	0.72	1.55	123.30	145.12	0.22	1.33	446	0.823	−0.08
		7.9	0.75	1.07	116.96	164.43	0.15	0.92	446	0.809	−0.038
		8.6	0.79	0.70	156.06	250.51	0.14	0.56	461	0.774	0.018
		9.0	0.74	0.43	168.35	335.29	0.10	0.33	466	0.735	0.135

Profile number	Soil group (WRB)	Depth	Al^{3+}	Fe$^{2+/3+}$	Mg^{2+}	Na^{+}	K^{+}	Ca^{2+}	CEC	Clay	Silt	Sand
		(cm)	(cmol + kg^{-1})	(cmol + kg^{-1})	(cmol + kg^{-1})	(cmol + kg^{-1})	(cmol + kg^{-1})	(cmol + kg^{-1})	(cmol + kg^{-1})	(%)	(%)	(%)
14	Kastanozem	15	0.00	0.06	0.69	0.00	0.30	4.19	6.31	4.80	19.39	75.81
		30	0.00	0.05	0.58	0.00	0.24	4.11	5.24	4.28	14.93	80.79
		50	0.00	0.03	0.32	0.00	0.22	3.24	3.39	4.32	28.69	66.99
		80	0.00	0.04	0.29	0.01	0.30	2.96	4.50	5.12	30.85	64.03
18	Arenosol	15	0.00	0.02	0.13	0.00	0.02	1.05	1.67	0.86	3.94	95.20
		30	0.00	0.01	0.11	0.00	0.02	0.61	0.62	0.69	2.52	96.79
		50	0.00	0.01	0.23	0.00	0.02	0.49	1.02	0.74	2.97	96.29
		80	0.04	0.01	0.15	0.00	0.01	0.30	0.90	0.81	3.24	95.95
19	Chernozem	15	0.00	0.44	3.52	0.10	0.76	22.19	35.88	12.67	68.23	19.10
		30	0.00	0.26	2.96	0.10	0.36	18.37	21.41	11.62	62.85	25.53
		50	0.00	0.26	3.00	0.11	0.31	15.63	21.53	10.99	64.91	24.10
		80	0.00	0.19	2.36	0.00	0.23	10.12	13.02	11.56	67.26	21.18
21	Kastanozem	15	0.00	0.10	0.56	0.00	0.28	6.30	8.06	7.56	29.60	62.84
		30	0.00	0.09	0.45	0.00	0.23	5.20	7.04	8.24	28.03	63.73
		50	0.00	0.07	0.32	0.00	0.26	3.89	4.60	5.61	36.95	57.44
		80	0.00	0.06	0.47	0.00	0.29	3.25	3.39	6.47	23.08	70.45

Profile number	Soil group (WRB)	pH	RM	TOC	HI	OI	PC	RC	Tmax	R-index	I-index
			(%)	(%)	(mg HC/g TOC)	mg CO2/g TOC)	(%)	(%)	(°C)	A3 + A4/100	log [(A1 + A2)/A3]
14	Kastanozem	8.5	0.21	0.72	116.13	166.08	0.10	0.62	423	0.726	0.020
		8.8	0.31	0.38	102.91	191.04	0.05	0.32	433	0.716	0.087
		8.8	0.19	0.23	162.72	287.68	0.05	0.18	429	0.724	0.107
		9.1	0.60	0.13	126.25	345.95	0.03	0.10	420	0.667	0.245
18	Arenosol	6.9	0.06	0.23	121.19	143.08	0.03	0.20	419	0.619	0.166
		6.5	0.03	0.11	115.61	146.69	0.02	0.10	418	0.628	0.237
		6.4	0.03	0.10	128.07	152.63	0.02	0.09	415	0.641	0.169
		5.5	0.02	0.06	93.21	195.14	0.01	0.06	405	0.604	0.399
19	Chernozem	8.4	1.06	5.09	76.31	111.71	0.48	4.61	425	0.682	0.039
		8.8	0.68	3.05	49.28	104.02	0.21	2.84	424	0.734	−0.051
		8.9	0.83	3.12	38.24	100.92	0.19	2.94	429	0.754	−0.060
		9.4	0.47	1.13	18.66	86.88	0.05	1.08	418	0.689	0.157
21	Kastanozem	8.9	0.52	1.00	81.05	162.71	0.11	0.89	440	0.773	−0.047
		8.9	0.38	0.65	85.56	206.39	0.08	0.56	446	0.770	−0.002
		9.0	0.33	0.45	89.76	250.08	0.06	0.38	447	0.752	0.073
		9.6	0.69	0.20	103.71	427.18	0.04	0.16	446	0.719	0.178

Profile number	Soil group (WRB)	Depth	Al^{3+}	Fe$^{2+/3+}$	Mg^{2+}	Na^{+}	K^{+}	Ca^{2+}	CEC	Clay	Silt	Sand
		(cm)	(cmol + kg^{-1})	(cmol + kg^{-1})	(cmol + kg^{-1})	(cmol + kg^{-1})	(cmol + kg^{-1})	(cmol + kg^{-1})	(cmol + kg^{-1})	(%)	(%)	(%)
23	Phaeozem	15	0.00	0.45	4.17	0.09	0.62	23.65	34.75	14.80	58.75	26.45
		30	0.00	0.27	2.63	0.00	0.25	15.64	23.95	11.41	59.91	28.68
		50	0.00	0.09	0.76	0.00	0.05	3.45	5.00	2.84	18.91	78.25
		80	0.00	0.09	0.92	0.00	0.07	4.25	6.75	5.20	34.07	60.73
27	Kastanozem	15	0.00	0.09	0.83	0.00	0.34	6.05	8.19	5.49	19.10	75.41
		30	0.00	0.09	0.78	0.00	0.20	5.45	7.23	6.64	33.18	60.19
		50	0.01	0.08	0.91	0.00	0.22	5.90	6.57	5.83	18.34	75.83
		80	0.00	0.09	1.19	0.00	0.24	5.36	7.92	5.10	28.46	66.44
29	Arenosol	15	0.00	0.02	0.14	0.00	0.05	1.65	2.00	0.76	3.31	95.93
		30	0.00	0.02	0.13	0.00	0.03	1.27	2.13	0.83	3.12	96.05
		50	0.00	0.02	0.16	0.00	0.03	1.54	1.68	0.71	2.76	96.53
		80	0.00	0.02	0.12	0.00	0.03	0.95	1.42	0.54	1.50	97.96
30	Kastanozem	15	0.00	0.23	3.29	0.02	0.40	14.75	22.69	20.76	53.09	26.15
		30	0.00	0.19	3.08	0.07	0.43	17.02	19.60	17.70	60.41	21.89
		50	0.00	0.20	4.41	0.06	0.45	16.07	19.14	15.69	52.50	31.81
		80	0.00	0.14	5.87	0.41	0.07	8.37	12.41	14.36	62.64	23.00

Profile number	Soil group (WRB)	pH	RM	TOC	HI	OI	PC	RC	Tmax	R-index	I-index
			(%)	(%)	(mg HC/g TOC)	mg CO2/g TOC)	(%)	(%)	(°C)	A3 + A4/100	log [(A1 + A2)/A3]
23	Phaeozem	6.5	1.14	6.02	71.20	115.18	0.55	5.47	419	0.593	0.181
		6.5	0.57	3.18	71.37	115.83	0.29	2.89	420	0.633	0.119
		7.1	0.16	0.28	40.30	96.92	0.02	0.26	337	0.584	0.385
		7.2	0.27	0.29	38.03	107.57	0.02	0.27	344	0.570	0.433
27	Kastanozem	7.6	0.16	1.04	86.02	151.69	0.12	0.92	420	0.654	0.120
		7.9	0.11	0.58	63.40	143.82	0.05	0.52	393	0.632	0.228
		8.4	0.20	0.22	70.23	215.94	0.03	0.19	353	0.620	0.335
		9.2	0.23	0.10	137.95	305.07	0.02	0.08	366	0.608	0.409
29	Arenosol	6.1	0.04	0.49	133.77	151.04	0.08	0.42	413	0.588	0.172
		7.0	−3.36	0.37	62.59	140.55	0.03	0.34	417	0.625	0.203
		7.3	0.03	0.31	55.11	118.47	0.02	0.29	424	0.653	0.193
		7.4	0.02	0.02	655.69	1471.63	0.02	0.00	396	0.614	0.345
30	Kastanozem	8.2	1.01	0.99	87.61	174.10	0.12	0.87	452	0.720	0.083
		8.2	1.09	0.67	83.92	241.02	0.09	0.58	406	0.690	0.122
		8.4	1.85	0.46	100.99	273.69	0.07	0.38	405	0.675	0.171
		8.9	1.74	0.17	103.71	335.60	0.03	0.14	371	0.635	0.289

Profile number	Soil group (WRB)	Depth	Al^{3+}	Fe$^{2+/3+}$	Mg^{2+}	Na^{+}	K^{+}	Ca^{2+}	CEC	Clay	Silt	Sand
		(cm)	(cmol + kg^{-1})	(cmol + kg^{-1})	(cmol + kg^{-1})	(cmol + kg^{-1})	(cmol + kg^{-1})	(cmol + kg^{-1})	(cmol + kg^{-1})	(%)	(%)	(%)
33	Calcisol	15	0.01	0.06	0.73	0.20	0.56	4.54	5.17	7.14	14.93	77.93
		30	0.00	0.07	0.72	0.00	0.39	4.99	7.14	4.00	21.66	74.34
		50	0.01	0.06	0.65	0.54	0.54	2.33	5.00	6.20	13.77	80.02
		80	0.01	0.05	0.42	1.96	0.81	1.88	3.32	10.63	21.69	67.68
34	Arenosol	15	0.02	0.01	0.05	0.00	0.01	0.18	0.42	0.55	0.61	98.84
		30	0.00	0.00	0.03	0.00	0.00	0.10	−0.02	0.46	0.62	98.92
		50	0.00	0.01	0.04	0.00	0.00	0.11	0.30	0.50	0.37	99.13
		80	0.00	0.01	0.02	0.00	0.00	0.06	0.43	0.65	1.63	97.72
35	Solonchak	15	0.00	0.13	1.03	4.64	0.47	2.55	11.59	12.32	57.68	30.00
		30	0.00	0.17	0.25	11.18	0.65	1.96	15.64	13.92	58.23	27.85
		50	0.01	0.20	0.12	17.88	0.86	0.88	19.08	10.72	66.66	22.62
		80	0.00	0.25	0.08	22.03	1.04	0.72	24.30	16.29	63.28	20.43
36	Solonetz	15	0.00	0.04	0.53	0.00	0.14	1.81	2.83	3.59	16.50	79.91
		30	0.00	0.04	0.32	0.02	0.09	0.60	1.90	2.55	13.97	83.48
		50	0.00	0.13	0.62	8.21	0.99	1.99	11.52	11.49	27.61	60.90
		80	0.02	0.13	0.02	11.83	0.87	0.34	12.24	12.35	22.63	65.02

Profile number	Soil group (WRB)	pH	RM	TOC	HI	OI	PC	RC	Tmax	R-index	I-index
			(%)	(%)	(mg HC/g TOC)	mg CO2/g TOC)	(%)	(%)	(°C)	A3 + A4/100	log [(A1 + A2)/A3]
33	Calcisol	8.7	0.13	0.58	194.24	264.53	0.14	0.44	437	0.720	0.024
		8.6	0.16	0.81	204.83	231.98	0.19	0.62	439	0.726	0.005
		9.1	0.12	0.35	190.55	334.75	0.09	0.26	438	0.726	0.039
		10.2	0.12	0.25	184.21	398.43	0.07	0.19	434	0.696	0.099
34	Arenosol	5.7	0.01	0.07	187.87	215.56	0.02	0.05	413	0.598	0.363
		6.6	0.01	0.03	329.41	171.50	0.01	0.02	400	0.600	0.447
		6.5	0.00	0.03	322.67	212.77	0.01	0.02	313	0.602	0.470
		6.5	0.01	0.01	588.96	139.42	0.01	0.01	437	0.610	0.475
35	Solonchak	9.4	0.32	0.57	93.55	147.97	0.07	0.50	452	0.729	0.202
		10.2	0.47	0.49	44.22	201.87	0.05	0.44	327	0.577	0.364
		10.2	0.47	0.46	24.27	200.37	0.04	0.43	325	0.570	0.463
		10.6	0.92	0.21	44.76	298.31	0.03	0.18	329	0.588	0.441
36	Solonetz	7.0	0.09	0.39	123.57	147.36	0.06	0.34	419	0.629	0.159
		8.2	0.05	0.14	141.40	136.19	0.02	0.12	405	0.600	0.268
		9.8	0.34	0.11	87.80	248.87	0.02	0.09	326	0.590	0.427
		11.3	0.37	0.10	52.06	245.58	0.01	0.09	328	0.598	0.457

Table A.2
Profile number associated to its soil type.

Profile number	Soil type
1	Kastanozem
2	Phaeozem
3	Solonetz
4	Kastanozem
5	Calcisol
6	Arenosol
7	Arenosol
8	Arenosol
9	Arenosol
10	Kastanozem
11	Arenosol
12	Arenosol
13	Kastanozem
14	Kastanozem
15	Arenosol
16	Kastanozem
17	Arenosol
18	Arenosol
19	Chernozem
20	Kastanozem
21	Kastanozem
22	Arenosol
23	Phaeozem
24	Arenosol
25	Phaeozem
26	Kastanozem
27	Kastanozem
28	Solonetz
29	Arenosol
30	Kastanozem
31	Kastanozem
32	Phaeozem
33	Calcisol
34	Arenosol
35	Solonchak
36	Solonetz

References

Acres, B.D., Rains, A.B., King, R.B., Lawton, R.M., Mitchell, A.J.B., Rackham, L.J., 1985. African Dambos: their distribution, characteristics and use. Z. Geomorphol., NF Suppl. Bd. 52, 63–86.

Amezketa, E., Aragües, R., 1995. Hydraulic conductivity, dispersion and osmotic explosion in arid-zone soils leached with electrolyte solutions. Soil Sci. 159, 287–295.

Aran, D., Maul, A., Masfaraud, J.-F., 2008. A spectrophotometric measurement of soil cation exchange capacity based on cobaltihexamine chloride absorbance. Geoscience 340, 865–871.

Behar, F., Beaumont, V., De Penteado, H.L.B., 2001. Rock-Eval 6 technology: performances and developments. Oil Gas Sci. Technol. Rev. IFP 2 (56), 111–134.

Blanchard, E., Albrecht, A., Bernoux, M., Brauman, A., Chotte, J.J., 2005. Organic matter and biofunctioning in tropical sandy soils and implications for its management. In: Hartmann, C., Chinabut, N., Noble, A., Niino, Y., Vearasilp, T., Polthanee, A., Poss, R. (Eds.), Management of Tropical Sandy Soils for Sustainable Agriculture. Proceedings. Khon-Kaen, pp. 224–241.

Burgess, J., 2006. Country Pasture/Forage Resource Profiles, Botswana. FAO, Rome.

Burrough, S.L., Thomas, D.S.G., 2008. Late quaternary lake-level fluctuations in the Mababe depression: middle Kalahari palaeolakes and the role of Zambezi inflows. Quat. Res. 69, 388–403.

Burrough, S.L., Thomas, D.S.G., Bailey, M., 2009. Mega-Lake in the Kalahari: a late Pleistocene record of the Palaeolake Makgadikgadi system. Quat. Res. 28, 1392–1411.

Butler, R.D., 1995. Zoogeomorphology: Animals as Geomorphic Agents. Cambridge University Press.

Cailleau, G., Braissant, O., Dupraz, C., Aragno, M., Verrecchia, E.P., 2004. Biologically induced accumulations of CaCO3 in orthox soils of Biga, Ivory Coast. Catena 59, 1–17.

Cailleau, G., Mota, M., Bindschedler, S., Junier, P., Verrecchia, E.P., 2014. Detection of active oxalate-carbonate pathway ecosystems in the Amazon Basin: global implications of a natural potential C sink. Catena 116, 132–141.

Ciesielski, H., Sterckeman, T., Santerne, M., Willery, J.-P., 1997. Determination of cation exchange capacity and exchangeable cations in soils by means of cobalt hexamine trichloride. Effects of experimental conditions. Agronomie 17, 1–7.

Correnblit, D., Corbara, B., Steiger, J., 2016. Biogeomorphic ecosystems within stressful and disturbed environments: a focus on termites and pioneer plants. In: Johnson, E.A., Martin, Y.E. (Eds.), A Biogeoscience Approach to Ecosystems. Cambridge University Press, pp. 456–474.

De Wit, P.V., Nachtergaele, F.O., 1990. Explanatory Note on the Soil Map of the Republic of Botswana. Soil Mapping and Advisory Services, Gaborone.

Diaz, N., Armitage, S.J., Verrecchia, E.P., Herman, F., 2019. OSL dating of a carbonate island in the Chobe Enclave, NW Botswana. Quat. Geochronol. 49, 172–176.

European Soil Data Center (ESDAC), 2014. Soil Atlas of Africa and its Associated Soil Map (Data). European Commission, Publications Office of the European Union, Luxembourg.

FAO, 2006. Guidelines for Soil Description. 4th edition. FAO, Rome.

Fynn, R.W.S., Chase, M., Roder, A., 2014. Functional habitat heterogeneity and large herbivore seasonal habitat selection in northern Botswana. S. Afr. J. Wildl. Res. 44, 1–15.

Grant, C.C., Scholes, M.C., 2006. The importance of nutrient hotspots in the conservation and management of large wild mammalian herbivores in semi-arid savanna's. Biol. Conserv. 130, 426–437.

Gutteridge, L., Reumerman, T., 2011. Okavango: A Field Guide. Southbound Field Guides.

Haddon, I.G., McCarthy, T.S., 2005. The Mesozoic–Cenozoic interior sag basins of central Africa: the late-cretaceous–Cenozoic Kalahari and Okavango basins. J. Afr. Earth Sci. 43, 316–333.

Haynes, G., 2012. Elephants (and extinct relatives) as earth-movers and ecosystem engineers. Geomorphology 157-158, 99–107.

Humphries, M.S., McCarthy, T.S., 2014. The role of airborne dust in the growth of tree islands in the Okavango Delta, Botswana. Geomorphology 206, 307–317.

IUSS Working Group WRB, 2014. World Reference Base for Soil Resources 2014: International Soil Classification System for Naming Soils and Creating Legends for Soil Maps. FAO, Rome.

Jones, C.R., 1980. The geology of the Kalahari. Botsw. Notes Rec. 14, 1–14.

Jones, B., 2002. Chobe Enclave, Botswana - Lessons Learnt from a CBNRM Project 1993–2002. CBNRM Support Project, Gaborone.

Jouquet, P., Lepage, M., Velde, B., 2002. Termite soil preferences and particle selections: strategies related to ecological requirements. Insect. Soc. 49, 1–7.

Jouquet, P., Bottinelli, N., Lata, J.-C., Mora, P., Caquineau, S., 2007. Role of the fungus-growing termite *Pseudacanthotermes spiniger* (Isoptera, Macrotermitinae) in the dynamic of clay and soil organic matter content. An experimental analysis. Geoderma 139, 127–133.

Jouquet, P., Traoré, S., Choosai, C., Hartmann, C., Bignell, D., 2011. Influence of termites on ecosystem functioning. Ecosystem services provided by termites. Eur. J. Soil Biol. 47, 215–222.

Kinabo, B.D., Atekwana, E.A., Hogan, J.P., Modisi, M.P., Wheaton, D.D., Kampunzu, A.B., 2007. Early structural development of the Okavango rift zone NW Botswana. J. Afr. Sci. 48, 125–136.

Kutsch, W.L., Bahn, M., Heinemeyer, A., 2009. Soil carbon relations: an overview. In: Kutsch, W.L., Bahn, M., Heinemeyer, A. (Eds.), Soil Carbon Dynamics: An Integrated Methodology. Cambridge University Press, Cambridge, pp. 1–15.

Legros, J.P., 2007. Les grands sols du monde. Presses Polytechniques et Universitaires Romandes, Lausanne.

Lehmann, J., Kleber, M., 2015. The contentious nature of soil organic matter. Nature 528, 60–68.

McCarthy, T.S., 2013. The Okavango delta and its place in the geomorphological evolution of southern Africa. S. Afr. J. Geol. 116 (1), 1–54.

McCarthy, T.S., Ellery, W.N., Dangerfield, J.M., 1998. The role of biota in the initiation and growth of islands on the floodplain of the Okavango alluvial fan, Botswana. Earth Surf. Process. Landf. 23, 291–310.

McCarthy, J., Gumbricht, T., McCarthy, T.S., 2005. Ecoregion classification in the Okavango Delta, Botswana from multitemporal remote sensing. Int. J. Remote Sens. 26 (19), 4339–4357. https://doi.org/10.1080/01431160500113583.

McCarthy, T.S., Humphries, M.S., Mahomed, I., Le Roux, P., Verhagen, B.Th., 2012. Island forming processes in the Okavango Delta, Botswana. Geomorphology 179, 249–257.

McNaughton, S.J., Banyikwa, F.F., McNaughton, M.M., 1997. Promotion of diet enhancing nutrients by African grazers. Science 278, 1798–1800.

Mendelsohn, J., Murray-Hudson, M., Wolski, P., Mosepele, K., 2010. Okavango Delta: Floods of Life. Raison, Windhoek.

Menichetti, L., Landi, L., Nannipieri, P., Katterer, T., Kirchmann, H., Renella, G., 2014. Chemical properties and biochemical activity of colonized and abandoned litter-feeding termite (Macrotermes spp.) mounds in chromic Cambisol area on the Borana plateau, Ethiopia. Pedosphere 24 (3), 399–407.

Moore, A., Cotterill, F.P.D., Main, M.P.L., Williams, H.B., 2007. The Zambezi river. In: Gupta, A. (Ed.), Large Rivers: Geomorphology and Management. John Wiley & Sons, Hoboken, pp. 311–332.

Mugerwa, S., Nyangito, M., Mpairwe, D., Nderitu, J., 2011. Effect of biotic and abiotic factors on composition and foraging intensity of subterranean termites. Afr. J. Environ. Sci. Technol. 5 (8), 579–588.

Munsell Color, 1994. Munsell Soil Color Charts. Munsell Color, New-York.

Muvengwi, J., Ndagurwa, H.G.T., Nyenda, T., Mbiba, M., 2016. Nutrient dynamics and plant assemblages of *Macrotermes falciger* mounds in a savanna ecosystem. Acta Oecol. 76, 13–21.

Orsini, L., Remy, J.C., 1976. Utilisation du chlorure de cobaltihexamine pour la détermination simultanée de la capacité d'échange et des bases échangeables des sols. Sci. Sol. 4, 269–275.

Preston, C.M., Schmidt, M.W., 2006. Black (pyrogenic) carbon: a synthesis of current knowledge and uncertainties with special consideration of boreal regions. Biogeosciences 3, 397–420.

Pricope, N.G., Gaughan, A.E., All, J.D., Binford, M.W., Rutina, L.P., 2015. Spatio-temporal analysis of vegetation dynamics in relation to shifting inundation and fire regimes:

disentangling environmental variability from land management decisions in a southern African transboundary watershed. Land 4, 627–655.

Rasse, D.P., Rumpel, C., Dignac, M.F., 2005. Is soil carbon mostly root carbon? Mechanisms for a specific stabilization. Plant Soil 269, 341–356.

Remmelzwaal, A., Van Waveren, E., 1988. Botswana Soil Database, Guidelines for Soil Profile Description. Soil Mapping Advisory Services, Gaborone.

Rowley, M.C., Estrada-Medina, H., Tzec-Gamboa, M., Rozin, A., Cailleau, G., Verrecchia, E.P., Green, I., 2017. Moving carbon between spheres, the potential oxalate-carbonate pathway of *Brosimum alicastrum Sw.; Moraceae*. Plant Soil 412, 465–479.

Rowley, M., Grand, S., Verrecchia, E.P., 2018. Calcium-mediated stabilization of soil organic carbon. Biogeochemistry 137, 27–49.

Ryan, P.C., 2014. Environmental and Low Temperature Geochemistry. John Wiley & Sons, Chirchester.

Schmidt, M.W.I., Torn, M.S., Abiven, S., Dittmar, T., Guggenberger, G., et al., 2011. Persistence of soil organic matter as an ecosystem property. Nature 478 (7367), 49–56.

Sebag, D., Verrecchia, E.P., Durand, A., 1999. Biogeochemical cycle of silica in an apolyhaline interdunal Holocene lake (Chad, N'Guigmi region, Niger). Naturwissenschaften 86, 475–478.

Sebag, D., Verrecchia, E.P., Cécillon, L., Adatte, T., Albrecht, R., et al., 2016. Dynamics of soil organic matter based on new rock-Eval indices. Geoderma 284, 185–203.

Sianga, K., Fynn, R., 2017. The Vegetation and Wildlife Habitats of the Savuti-Mababe-Linyanti Ecosystem, Northern Botswana. vol. 59. KOEDOE, p. a1406.

Skarpe, C., Arrestad, P.A., Andreassen, H.P., Dhillion, S.S., Dimakatso, T., et al., 2004. The return of the giants: ecological effects of an increasing elephant population. Ambio 33 (6), 276–282.

Stockmann, U., Adams, M.A., Crawford, J.W., Field, D.J., Henakaarchchi, N., et al., 2013. The knowns, known unknowns and unknowns of sequestration of soil organic carbon. Agric. Ecosyst. Environ. 164, 80–99.

Stoops, G., 2003. Guidelines for Analysis and Description of Soil and Regolith Thin Sections. Soil Science Society of America, Inc, Madison, Wisconsin, USA, p. 184.

Thomas, G.W., Hargrove, W.L., 1984. The chemistry of soil acidity. In: Adams, F. (Ed.), Soil Acidity and Liming. American Society of Agronomy Inc, Madison, pp. 3–56.

Troeh, R.R., Thompson, L.M., 2005. Soils and Soil Fertility. 6th ed. Wiley-Blackwell, Iowa.

Verrecchia, E.P., 1990. Lithodiagenetic implications of the calcium oxalate-carbonate biogeochemical cycle in semi-arid calcretes, Nazareth, Israel. Geomicrobiol J. 8 (2), 89–101.

Verrecchia, E.P., Braissant, O., Cailleau, G., 2006. The oxalate-carbonate pathway in soil carbon storage: the role of fungi and oxalotrophic bacteria. In: Gadd, G.M. (Ed.), Fungi in Biogeochemical Cycles. Cambridge University Press, Cambridge, pp. 289–310.

Wang, L., D'Odoricoa, P., Ringrose, S., Coetzee, S., Macko, S.A., 2007. Biogeochemistry of Kalahari sands. J. Arid Environ. 71, 259–279.

Wong, V.N.L., Greene, R.S.B., Dalal, R.C., Murphy, B.W., 2010. Soil carbon dynamics in saline and sodic soils: a review. Soil Use Manag. 26, 2–11.

Yuan, B.C., Li, Z.Z., Liu, H., Gao, M., Zhang, Y.Y., 2007. Microbial biomass and activity in salt affected soils under arid conditions. Appl. Soil Ecol. 35, 319–328.